Master of Science Thesis

Intensity Modulated Radiotherapy Treatment Planning with OTP/TMS for Head&Neck Carcinomas in the ARTSCAN study

Petra Ambolt

Supervisors:
Per Nilsson & Tommy Knöös
Department of Radiation Physics
Lund University Hospital

Department of Medical Radiation Physics
The Jubileum Institute
Lund University, 2004

Ny metod för att behandla cancer med strålning

Cancer är en otrevlig sjukdom, som drabbar många människor. Man söker ständigt nya och bättre sätt att bota patienter eller åtminstone lindra sjukdomens framfart. Ett vanligt sätt att behandla cancer är med strålning. Strålningen kan bestå av sk *fotoner*. Fotoner är samma slags partiklar som t.ex. vanligt ljus. Skillnaden är att de fotoner som används vid strålbehandling av cancer har högre energi och kan ta sig in i kroppen och förstöra celler. Man vill att strålningen bara ska förstöra tumörceller och inte celler i friska organ som ligger nära tumören. Detta är dessvärre inte så lätt att åstadkomma, men man försöker minimera biverkningarna. Biverkningar som inte är livshotande får ofta accepteras eftersom man annars riskerar att låta tumören överleva. Exempelvis förlorar patienter med cancer i huvud-hals området ofta sin salivproduktion helt pga strålskador på spottkörtlarna. Detta är ett stort problem för patienterna, som därmed får svårighet att tugga och svälja. Smaken försvinner och risken för tandlossning ökar. Det har dock visat sig att patienten kan få tillbaka sin salivproduktion om man kan ge lite mindre strålning till den ena av spottkörtlarna.

Det finns nu en ny metod inom strålbehandling, som kallas ***IMRT***, och som innebär att man på ett bättre sätt kan koncentrera strålningen till tumören utan att skada känsliga organ i närheten. IMRT står för ***I***ntensitets***m***odulerad ***R***adio***t***erapi. Radioterapi betyder strålbehandling och intensitetsmodulerad innebär att man delar upp sitt strålfält i många mindre fält, där man strålar olika mycket på varje litet fält. Resultatet blir ett strålfält med olika intensitet på olika ställen, därav ordet intensitetsmodulerad. Hur mycket man ska stråla på varje ställe låter man en dator räkna ut. Man specificerar hur mycket strålning man vill ge till tumören och anger samtidigt hur mycket friska organ tål. Dator-programmet räknar sedan ut på vilket sätt man bäst kan uppnå det resultat man vill.

Målet är att Universitetssjukhuset i Lund ska kunna använda sig av IMRT inom en snar framtid, men innan detta är möjligt måste många tester utföras. Olika sjukhus har ofta olika utrustning och de metoder som fungerar bäst på ett sjukhus är inte nödvändigtvis de bästa på ett annat. Syftet med det här arbetet var att ta reda på om man, med hjälp av IMRT och den utrustning som finns här, kan ge patienter med cancer i huvud-hals området en bättre behandling än med de metoder som används idag. Framför allt vill vi undvika förlust av salivproduktionen. Arbetet har visat att det går att ge mindre strålning till en av spottkörtlarna, men tyvärr så leder det oftast till att tumören inte får riktigt så mycket strålning som man önskar. Detta beror dock på vilken utrustning man använder. Tester med annan utrustning visade att IMRT definitivt ger en bättre behandling för de här patienterna. Förhoppningen är ändå att efter fler tester och förbättringar kunna börja använda IMRT i Lund inom kort.

TABLE OF CONTENTS

Abstract

Purpose: The aim of this study was to investigate whether inversely planned intensity modulated radiation therapy (IMRT), using the clinical radiotherapy equipment at hand in our department, renders any advantages regarding dose distribution over conventional radiotherapy for head and neck cancer patients in the ARTSCAN (Accelerated RadioTherapy of Squamous cell Carcinoma in the head And Neck) study, with special consideration to parotid sparing.

Materials and Methods: The treatment plans were optimized for an Elekta SL*i* accelerator using the Oncentra Treatment Planning (OTP) system (version 1.2) from Nucletron for the inverse planning of the patient cases. For the final forward calculations, the Helax-TMS ver 6.1A, SP 1, (Nucletron) was used. The treatment planning systems (TPS), as well as the Elekta accelerator, only support step-and-shoot IMRT technique. A total of five patients have been used, all diagnosed with squamous cell carcinoma of the tonsil. The patients had all prior to this work received treatment according to the ARTSCAN protocol using conventional planning and treatment technique. The influence of different planning parameters (such as number of fields, number of intensity levels and segments per beam) on the dose distribution was investigated. The dose-volume distribution aimed for are according to the ARTSCAN protocol, i.e. 95 – 105 % of the prescribed dose (46 Gy in 23 fractions) to the planning target volume (PTV), including bilateral neck nodes, and a maximum spinal cord dose of 45 Gy (allowing for additional dose contribution from the boost treatment). Furthermore, the mean dose to the contralateral parotid gland was decided to be kept below 26 Gy to avoid permanent xerostomia. The treatment plans were evaluated in terms of physical quantities based on dose–volume histograms and isodose distributions. The IMRT plans were compared to the existing conventional plans (used for treatment of the patients) and also to plans optimized on the same patient at the Department of Radiation Physics in Umeå (using the same treatment planning equipment as in this study) and in Göteborg (using different planning and delivering techniques).

Results: It is shown that the optimal IMRT settings for the given situation, is to use seven coplanar beams, separated by equal angles, ten intensity levels and a maximum of ten segments per beam. The dose-volume constraints for the PTV need to be stricter than the 95 – 105 % aim and the organ at risk (OAR) constraints must usually be set to a lower level than the actual tolerance doses. The IMRT plans show slightly worse PTV coverage and a larger standard deviation than the conventional plans, but the doses to the organs at risk are on the other hand lower. It is also shown that the quality of an IMRT plan is strongly dependent on the equipment used. The plan optimized with the other equipment showed better dose conformity and lower standard deviation as well as lower normal tissue doses.

Conclusions: This work shows the possibilities of normal tissue sparing using IMRT. The contralateral parotid gland mean dose is easily kept below the threshold dose of 26 Gy in the IMRT plans. The spinal cord maximum dose is also usually lower as compared to the conventional plans. This normal tissue sparing is however always achieved at the cost of target coverage. The use of a different TPS may produce superior treatment plans, which is shown to be true in one particular case.

1. Introduction

Approximately 1000 patients are yearly diagnosed with head and neck carcinomas in Sweden. This corresponds to roughly 2 % of all cancer. The incidence of this diagnose is expected to increase with 25 % within the next decade (SBU 2003). External radiotherapy is an important treatment modality for these patients (SBU 1996). Almost all head and neck patients receive radiotherapy, from which 90 % with intention to cure (SBU 2003). Most head and neck tumours are squamous cell carcinomas which require high absorbed dose to the tumour to achieve local control. However, severe side-effects (mainly late) are dose limiting, resulting in an average total dose of 66-70 Gy depending on tumour site and treatment traditions at different clinics (SBU 2003). Regional neck-node metastases are frequent in this group of patients. Leaving a clinically tumour free lymph node station untreated results in a high probability of metastases in the ipsilateral side within two years. Metastases in the contralateral neck nodes have been seen in almost 50 % of the cases within the same period of time (SBU 1996). It is therefore common to include the neck nodes on both sides in the target volume. It has been shown that an absorbed dose of 50 Gy will eliminate 90 % of the subclinical disease (SBU 1996).

The anatomy in the head and neck region is very complex with a variety of radiosensitive organs, for example the spinal cord and the parotid glands (see Figure 1). These organs at risk are often located in close proximity to or even partly inside the planning target volume. This gives rise to a complex geometry, making it hard to achieve the dose distribution aimed at within the target volume without exceeding tolerable doses to the organs at risk, using conventional radiotherapy techniques.

Acute side-effects, for instance skin erythema, are usually considered acceptable except when a patient's medical condition is already poor or when the severity of the side-effect will cause irreversible normal tissue changes. The spinal cord is considered to be a serially organized organ (Källman et al, 1992), i.e. an organ with low dose-volume dependence and, hence, damage to this organ is critically dependent on the given maximum dose. Late side-effects such as radiation myelitis have been reported after approximately 48 Gy depending on fractionation scheme (e.g. Horiot et al, 1997). Other, less severe side-effects might be considered acceptable if tumour control can be achieved. For instance, head and neck patients with bilateral neck-nodes included in the target volume generally receive parotid gland doses high enough to permanently eradicate the organ function, thus leading to reduction of salivary flow causing dryness of the mouth.

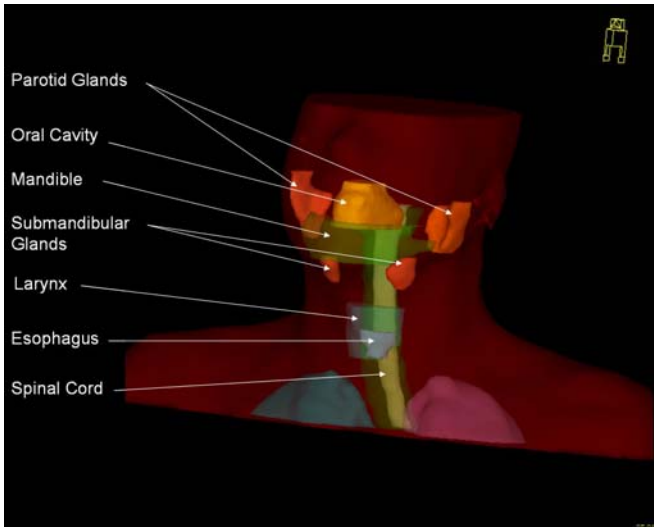

Figure 1. Example of organs at risk in the head and neck region.

Such radio-induced xerostomia is usually permanent and severe, leading to oral discomfort, difficulty in chewing and swallowing, altered taste, altered speech, and chronic changes in the oral flora, which increase the risk of dental caries, soft tissue ulceration, and esophagitis. The tissue architecture of the parotid glands is considered to be parallel (Eisbruch et al, 1999), i.e. an organ with a large dose-volume dependence. Thus even if part of the organ receives a high dose the organ function might still be preserved. Whether the xerostomia will be irreversible, and the severity of the condition, is thus related to the mean dose rather than the maximum dose received. A mean dose threshold has been suggested for parotid saliva flow rates. This threshold dose is around 26 Gy. Glands receiving a mean dose below that threshold exhibit a time-related recovery, whereas a higher mean dose generally implies permanent xerostomia (Eisbruch et al, 1999). This condition will considerably decrease quality of life, hence sparing of the parotid glands would be a significant gain for the patients. However, the ipsilateral parotid is normally located entirely inside the planning target volume (ICRU, 1993) and will therefore receive the same dose as the target volume. The contralateral parotid, on the other hand, is generally located only partly inside the target volume, and thus accessible for sparing.

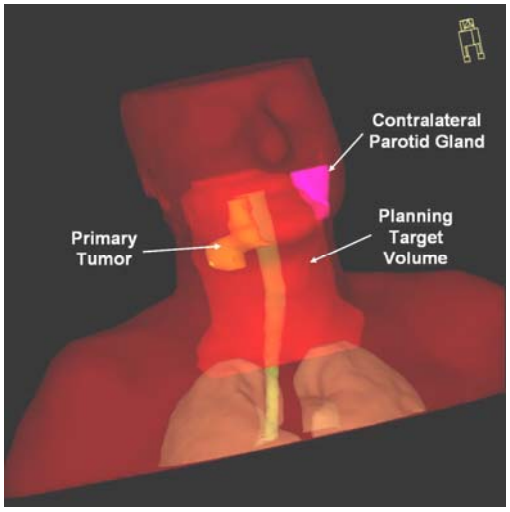

Figure 2. A 3D view of the primary tumour and the planning target volume overlapping the contralateral parotid gland.

Sparing of the parotid gland without compromising target coverage can potentially be accomplished using intensity modulated radiotherapy (IMRT) as first proposed by Brahme et al, 1982. IMRT is a fairly recent technical advancement offering clinical benefits that might not be achievable with conventional radiotherapy. The fundamental idea of radiotherapy is to enable delivery of a conformal high radiation dose to the target volume while sparing nearby critical structures. With IMRT this can be achieved even for tumours with concave regions. This is realized using the multileaf collimator (MLC) of the accelerator to form smaller sub-beams which superimposed shape a non-uniform field. The photon fluence distribution for each treatment field is in general accomplished by an inverse treatment planning process. In conventional radiotherapy treatment planning, the treatment plan is created in a trial and error process of choosing beam angles and beam shapes, beam weights, wedges, etc. Inverse planning implies defining the dose distribution to be deposited in the patient and then letting the treatment planning system calculate the necessary incident beam profiles (see Figure 3). In general, there is no straightforward solution of the inverse problem due to the physical properties of x-rays. Therefore, the inverse problem has to be solved using an optimization algorithm. For this, an objective function is used. In the next step, the beam fluence is modified. If the value of the objective function is reduced this plan is accepted, otherwise another modification is performed. This iteration process is continued until a minimum is reached.

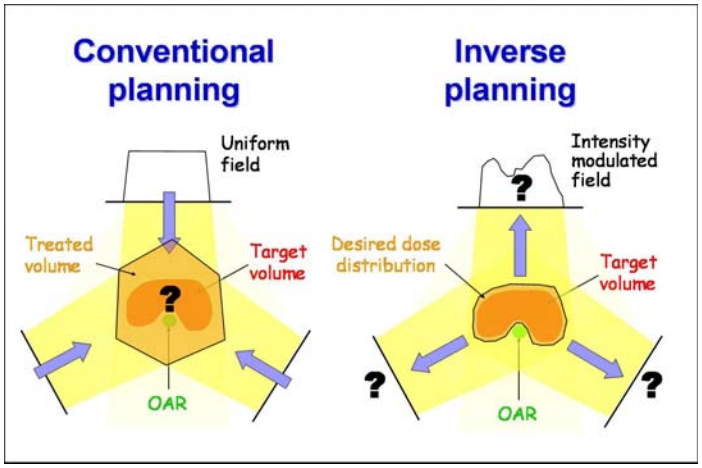

Figure 3. Conventional (left) vs. inverse planning (right). Redrawn from Bortfeld et al, 2002.

IMRT treatment plans in general use more beams than conventional plans. It has been shown that the dose gradients around the target volume and critical structures will increase with increasing number of field (Samuelsson et al, 2003a). These steeper dose gradients in the treatment plan will increase the sensitivity to set-up errors with regard to the critical structures (Samuelsson et al, 2003b). The importance of accurate patient immobilization therefore becomes increasingly apparent. Systematic set-up errors can potentially produce normal tissue overdosing in IMRT plans (Manning et al, 2001). ICRU Report no 62 (ICRU 1999) recommends the use of planning organ at risk volumes (PRV) to allow for organ movement and setup uncertainties. This will however compromise the target coverage when the critical structure is located partly inside or close to the planning target volume, and hence the use of a PRV in this case will have to be decided upon an individual patient basis.

Head and neck carcinomas are well suited for IMRT for several reasons. The fact that squamous cell carcinomas require rather high absorbed dose to achieve local control, and the complex geometry in the head and neck region with critical radiosensitive structures in the proximity of the target volume, are amongst the dilemmas for conventional radiotherapy treatment planners. Furthermore, a good patient immobilization is often achieved in the head and neck (see Figure 4). In addition to this, the organ movements in this region are small, providing a geometrical organ precision superior to that for many other cancer sites.

Figure 4. Example of individualized patient immobilization (medtec.com).

ARTSCAN (Accelerated RadioTherapy of Squamous cell Carcinoma in the head And Neck) is an ongoing Swedish randomized controlled study on head and neck cancer. The aim of the study is to compare radical conventionally fractionated radiotherapy with accelerated fractionation with respect to local control, survival, quality of life, and morbidity. The patients treated within this study usually suffer from severe chronic xerostomia. Some clinics in Sweden have recently started to use IMRT for patients in this study. The patients that would benefit most from IMRT are patients with carcinoma in the tonsil with bilateral neck-nodes since, in these cases, the spinal cord is partly surrounded by the concave planning target volume (PTV) and the contralateral parotid gland accessible for normal tissue sparing (see Figure 5).

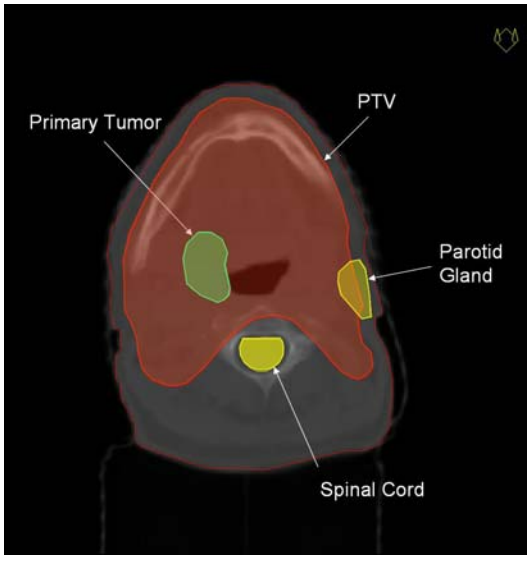

Figure 5. A tranversal cross section at the level of the mandible showing the primary tumour in green, the planning target volume in red and the organs at risk in yellow.

The aim of the present work is to investigate whether inversely planned IMRT, using the clinical radiotherapy equipment at hand in our department (OTP and Helax-TMS[1] treatment planning systems connected to Elekta SL*i* accelerators[2] via Oncentra-Visir[1]), renders any advantages regarding dose distribution over conventional radiotherapy for this group of head and neck cancer patients in the ARTSCAN study, with special consideration to parotid sparing.

[1] Nucletron B. V., Veenendaal, The Netherlands

[2] Elekta Oncology Systems, Crawley, UK

2. Inverse Treatment Planning

An important step in IMRT is the optimization, or the inverse planning. Based on manually preset beam ports and a number of constraints for the target and normal tissues, an optimization algorithm in the treatment planning system (TPS) calculates the optimum photon fluence ("intensity") distribution for each treatment field. Inversely planned IMRT is in practice usually not an automatic process as shown in Figure 6.

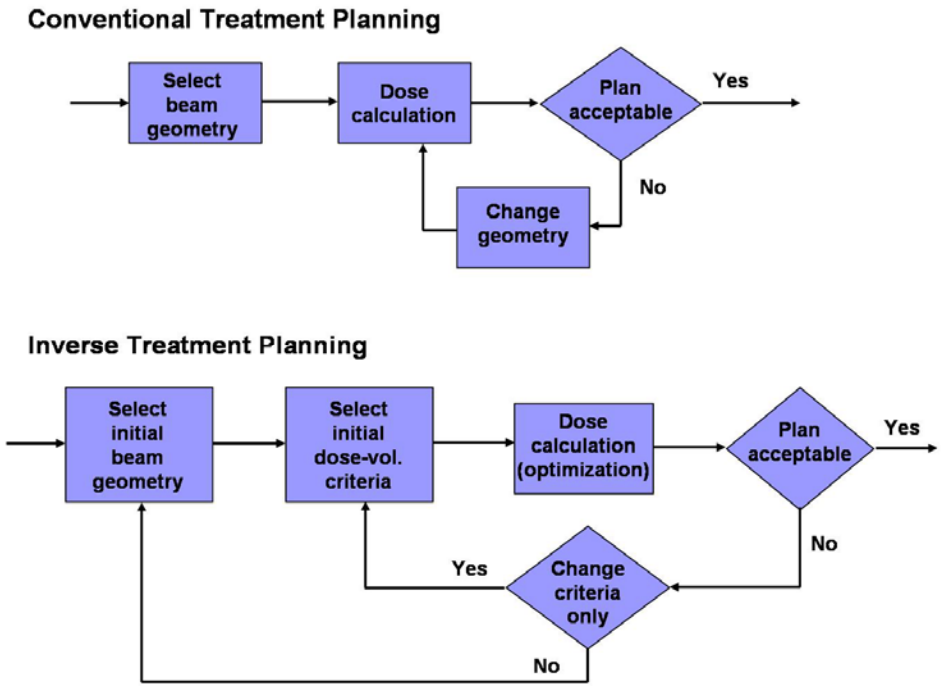

Figure 6. A schematic flowchart of conventional treatment planning vs. inverse treatment planning.

The optimum photon fluence distribution is calculated by minimizing an objective function (see Figure 7). This function can either be based on physical indices, i.e. absorbed dose (Oelfke et al. 2001) or biological indices, e.g. tumour control probability (TCP) and normal tissue complication probability (NTCP) models (Brahme et al. 2001). To this day mainly the former is in clinical use, primarily due to the lack of reliable input data for the biological models. The dose-based objective function typically includes target prescription dose, target dose homogeneity and dose-volume constraints for the organs at risk (OAR). Objective functions of quadratic forms are the most commonly used, primarily due to their mathematical simplicity (Figure 7). It can be shown that dose-volume based objective functions most likely contain multiple local minima as seen in

Figure 7 (Deasy, 1997). It should be noted that the numerical value of an objective function normally has no fundamental physical relevance.

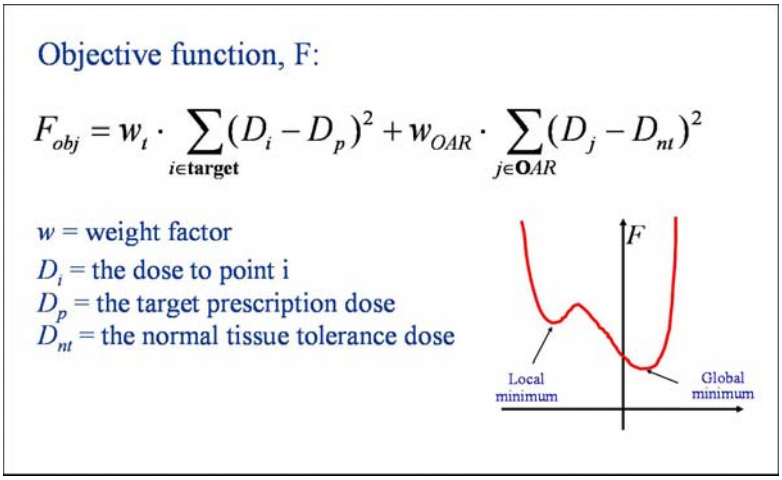

Figure 7. Example of a dose-difference based objective function of quadratic form.

2.1 Optimization Algorithms in general

Optimization algorithms are normally limited to refining existing treatment plans by determining e.g. intensity maps and suitable beam weights, i.e. the planner usually decides upon the number of fields and gantry angles before the optimization. There are a number of different requirements on an optimization algorithm, e.g. it is desired that the algorithm is fast and that the result found is actually the global minimum. Requirements like these often imply the use of different algorithms in a treatment planning system, i.e. one algorithm might be used for shaping the segments, another one for the main optimization and maybe a third one for optimizing gantry angles (not an option in the TPS used for this study).

There are in principle two types of iterative algorithms available to perform the search for the global minimum of the objective function: the stochastic and the deterministic approach. Stochastic algorithms rely on random sampling. The most well known is the *simulated annealing* algorithm, which simulates the slowly decreasing temperature of a thermalized system reaching its ground state (Webb, 1989). The ray or beamlet weights are slightly changed at each step of the iteration. The change is automatically accepted if the score function decreases. If the score increases the change is accepted with a probability of $e^{-\Delta F/kT}$, where ΔF is the change in score, k is the Boltzmann constant and T is the "temperature" at this stage. The fact that the algorithm might accept changes that worsen the dose distribution makes the simulated annealing a relatively inefficient method, but the advantage is that this method has the potential to escape from local minima (Chui and Spirou, 2001).

Deterministic algorithms are usually iterative methods based on either dose difference or dose ratios. At each iteration step the solution is updated based on the dose difference (ratio) between the calculated and the prescribed dose. The gradient method is a common deterministic algorithm, where the solution is updated along the gradient of the objective function and the updates are based on dose difference. Deterministic algorithms are faster than simulated annealing but will always proceed to find the closest minimum, i.e. they cannot avoid getting trapped in local minima. This might not be a clinical problem, however, since it has been shown that the existence of multiple local minima in general does not affect the outcome of optimization in any clinically significant way when using the gradient method (Wu et al, 2002).

2.2 MLC Segmentation (Leaf Sequencing)

IMRT requires that the non-uniform photon beams determined by the TPS can be delivered by the accelerator. This can be realized by introducing either compensator filters (beam intensity modulators) into the beam or using the multileaf collimator (MLC). The former basically implies placing a filter material of various thickness between the source and the patient, hence generating an intensity modulated field. This is the earliest form of intensity modulated radiotherapy but is not a concern of this work and will thus not be further discussed. There are two different delivery methods in MLC-based IMRT, dynamic MLC and static leaf sequence technique. In the dynamic MLC (dMLC) mode the leaves move continuously, with different speed, during radiation (Convery and Rosenbloom, 1992). The static leaf sequence technique implies superposition of several smaller beam segments (Galvin et al, 1993).

For each requested gantry angle, the calculated 2D photon fluence distribution has to be reformatted to a distribution that can be realized utilizing the MLC. The reformatted distribution is discrete and the resemblance to the photon fluence distribution will depend on the number of intensity levels (see Figure 8). The matrix cell size is approximately 10x10 mm^2 because of the design of the MLC (Saw et al, 2001). The complex non-uniform field described by the fluence map is broken down into segments of uniform fields that can be implemented by the MLC. It is of course of importance that the reformatted fluence map is as close as possible to the optimal dose distribution produced by the initial optimization algorithm.

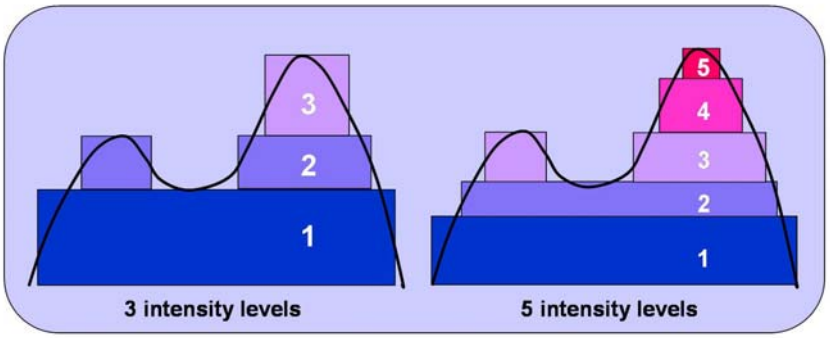

Figure 8. Example of a calculated 1D fluence distribution (black solid curve) and its discretized form for two different number of intensity levels.

Static leaf sequences are normally referred to as the step-and-shoot technique. In this method the leaves are stationary as the dose is delivered. Decomposing an intensity-modulated field into a series of segments can be done in many different ways. The treatment time is strongly dependent on the total number of segments, so the smallest number of segments is desirable. It should be noted, however, that this should be the result of an effective leaf sequencing algorithm. One way of reducing the number of segments would otherwise be to decrease the number of intensity levels, which would result in less precision in dose delivery. There is always a compromise between the precise dose delivery and the delivery time (Saw et al, 2001).

The use of dynamic leaves is commonly accomplished by letting the MLC form a window that moves continuously in one direction and is therefore usually referred to as the sliding window technique. The intensity map can be produced either by varying the leaf speed or the dose rate, the former being the more flexible method. The maximum intensity difference will then be dependent on the maximum and minimum speed allowed for the leaf movement. Using the dMLC method usually offers shorter treatment time than the step-and-shoot technique. However, whether to apply dMLC or the step-and-shoot technique is not always a choice of the user since in some configurations the accelerator and/or TPS only support one of the techniques.

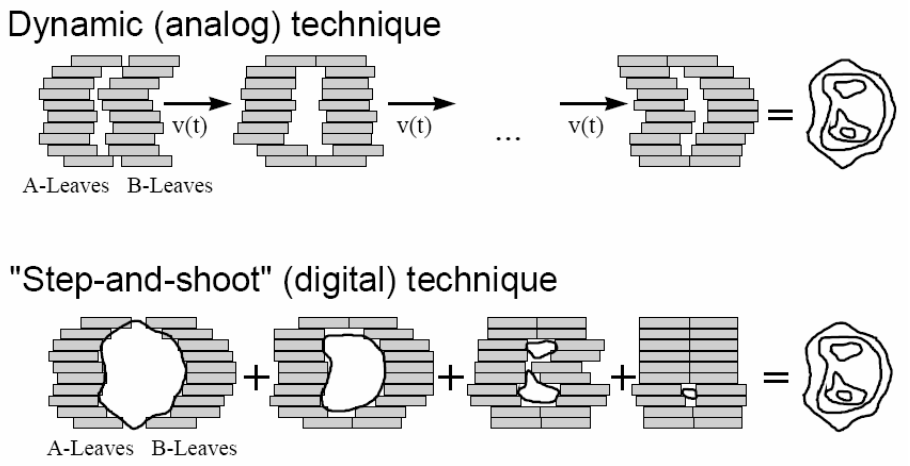

Figure 9. dMLC vs. the step-and-shoot technique (from Bortfeld et al, 1999). In dMLC the leaves move continuously during the radiation to create the final intensity map, whereas the step-and-shoot technique consists of a number of segments that superimposed create the intensity map.

2.3 The Oncentra Treatment Planning (OTP) IMRT Module

The OTP IMRT module consists of two different optimization loops. In the first one, the shapes of the segments are created and in the second one, the main optimization, the monitor units for each segment are determined. The TPS uses the same dose-volume based objective function for both optimization loops. The initial guess is generated by producing a projection of the target volume (with some margin) at the isocenter plane for each field. Homogeneous fluence matrices are created, the dose distribution for this case is calculated and the objective function can be evaluated.

A description of the IMRT module can be found in the TPS documentation (MDS Nordion). Only a condense version of the IMRT module will be given in this report.

2.3.1 The Objective Function

The TPS supports optimization of a dose and dose-volume based objective function which takes variable bounds into account. The principle in defining the objective function for dose plan optimization has been to find the optimal compromise between target dose coverage and critical structure sparing, based on an importance classification of volumes made by the user. The objective function, F, has been defined as

$$F(\mathbf{D}) = T(\mathbf{D}) + R(\mathbf{D})$$

where T is the target term, R is the organ at risk term and $\mathbf{D}$ is the calculated dose distribution defined as

$$\mathbf{D} = \bigcup_{\mathbf{m}} \bigcup_{\mathbf{n}} D_{m,n}$$

where $D_{m,n}$ is the absorbed dose in the n:th voxel in the m:th volume of interest. The target and organ at risk terms are defined as

$$T(\mathbf{D}) = \sum_{\mathbf{m}\in\mathbf{T}} w_m \cdot \delta_m(\mathbf{D}) \cdot C_m(\mathbf{D})$$

$$R(\mathbf{D}) = \sum_{\mathbf{m}\in\mathbf{R}} w_m \cdot \delta_m(\mathbf{D}) \cdot C_m(\mathbf{D})$$

where w_i is a constraint weight factor defined by the user. This factor ranks the relative importance of fulfilling the constraints for a certain VOI. The parameter δ_m is the squared deviation from the preferred dose. This is an integral where the contribution to δ_m from a voxel with dose $D_{m,n}$ is proportional to $(D_{m,n} - \hat{D}_m)^2$, where $\hat{D}_m$ is the mean value of the highest and lowest dose value in the target volume and the minimum value for volumes defined as organs at risk. Also, in a critical structure, the contribution to δ_m from a voxel where $D_{m,n} < \hat{D}_m$ is zero. This means that the factor δ_m will help avoiding overdosage in critical structures while it will enforce homogeneous dose in the target. C_m is a violation factor for the m:th VOI. It has a value of zero if all the constraints for the VOI are fulfilled. C_m then increases with increasing violation in volume fulfilment, finally reaching its maximum value of unity.

If all dose-volume constraints are satisfied, the objective function will assume the value zero which will stop the optimization process. This case does not necessarily correspond to the best plan available, but merely implies that all constraints are fulfilled. If the algorithm fails to fulfil all constraints simultaneously, the result will be a compromise between target coverage and sparing of organs at risk. It should be noted that this compromise not necessarily is clinically beneficial. It is recommended by the TPS vendor to set realistic dose-volume constraints that are at least approximately achievable for optimal performance.

2.3.2 Modulation Segmentation

The used TPS only supports segmental multileaf modulation, i.e. the step-and-shoot technique. The process of determining the optimal MLC and jaw positions is performed in an initial step of the optimization. To obtain modulation matrices, a preliminary optimization is first performed using the so called L-BFGS-B algorithm (Byrd et al, 1995). This algorithm provides a smoother fluence variation than the algorithm used for the main optimization. Smoothness is required to obtain a smaller number of sub-beams. Based on the leaf boundaries and the location of the target, modulation matrices for the different beams are initialized. The objective function, F, is then used to optimize the modulation matrices and the dose contribution from each pixel is determined. The head scatter component is not considered in this step.

When the preliminary optimization is completed, the modulation matrices for the different beams are discretized to a number of intensity levels pre-specified by the user. Continuous areas are identified in the resampled matrices. The leaf positions for the different sub-beams are determined using a sliding window technique for each pair of

leafs. This means that the leftmost leaf is positioned at a location where the subsequent pixel value is larger than the previous, whereas the rightmost leaf will be located where there is a decrease in modulation between consecutive pixels. The lower jaws and the back-up collimator (se Figure 15, page 19) are then positioned so that the open area will be as small as possible without blocking the field.

When the sub-beams have been generated, the TPS will first simply omit the sub-beams violating the MLC limitations for the specific accelerator used. Examples of MLC limitations are minimum separation between the leaves in a leaf pair or minimum separation between a leaf in one leaf bank and an adjacent leaf in the opposing leaf bank (see Figure 10). The limitations are unit-specific and are defined in the treatment unit database of the TPS. Also, sub-beams that are considered sufficiently equivalent are merged into one single sub-beam. Here, sufficiently equivalent means that the leaf positions between sub-beams are differing at most a user-specified distance. The number of sub-beams might be further reduced in view of the fact that the user is able to specify the total number of sub-beams allowed per beam and also a minimum MU value for each sub-beam. In the first case, the sub-beam with the smallest area is simply removed. In the latter case, a sub-beam with a MU value below half of the requested minimum will be removed whereas a MU value between half and whole of the requested value will result in an increase of the sub-beam MU value up to the minimum value. This procedure, however, will obviously be performed first after the main optimization (where the beam MUs are optimized).

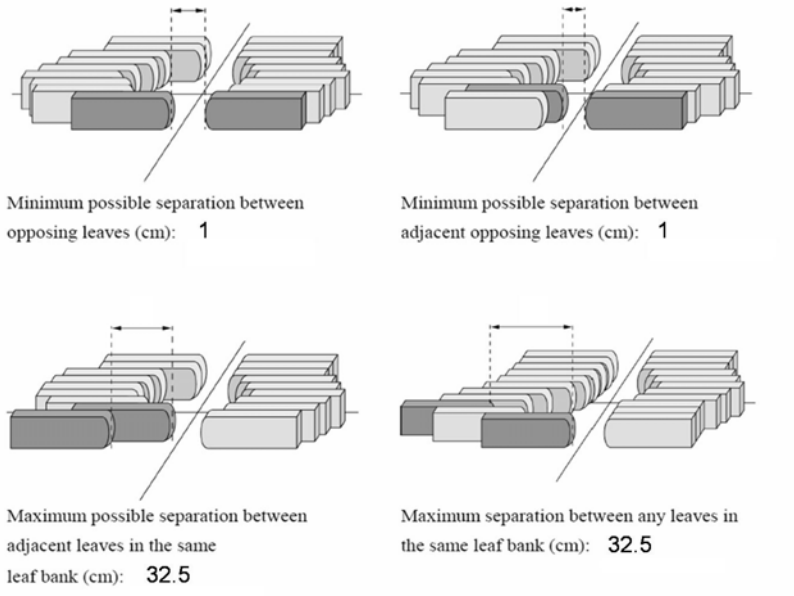

Figure 10. The constraints of the Elekta MLC.

2.3.3 The Optimization Algorithm

The optimization algorithm in the TPS is an implementation of a large-scale generalized reduced gradient algorithm (LSGRG2). The gradient of the objective function is reduced using Lagrange multipliers. A search direction is chosen based on the gradient and a line search along this direction is performed using quadratic interpolation. The solution resulting from the line search is used as the new input vector. During each iteration step, the total dose has to be calculated in order to obtain the value of the objective function. When the fractional change in objective function is less than 0.001 for three consecutive steps, the optimization is terminated. The optimization will also terminate if certain conditions are satisfied to within some convergence tolerance (the so called Karush-Kuhn-Tucker conditions). The Karush-Kuhn-Tucker factor gives an approximate value of how close to a local minimum the solution is, and when this factor is considered sufficiently small, the optimization will stop (Smith and Lasdon, 1992).

When the optimization has converged to an optimal solution, the TPS performs a final dose calculation. The user can choose to use either the pencil-beam or the collapsed-cone algorithm for this final dose results. During optimization, however, the pencil-beam algorithm is used to shorten the calculation time. During the final dose calculation the head scatter is also taken into account.

2.3.4 Dose-Volume Constraints and Weight Factors

In the TPS the following dose-volume constraints for the target volume need to be specified. The numbers in parenthesis are referring to Figure 11 below.

- Minimum Dose (Gy) – all parts of the target must receive at least this dose (**1**).
- Prescription Dose (Gy) – defines the ideal dose for the entire target. If possible, all parts of the target should receive this dose (**2**).
- Under Dose Volume (%) – defines how large a fraction of the target volume may receive lower dose than the prescribed dose (**3**).
- Limit Dose (Gy) – defines the highest acceptable dose for any part of the target (**4**).

For the organs at risk (OAR) the following dose-volume constraints need to be specified:

- Full Volume Dose (Gy) – defines the highest acceptable dose to the whole OAR volume. Less than 100 % may receive more than Full Volume Dose (**5**).
- Maximum Dose (Gy) – defines the highest acceptable dose to a specified portion of the OAR volume. Only a fraction of the OAR volume may receive the maximum dose (**6**).
- Over Dose (%) – defines how large a fraction of the OAR volume may receive higher dose than the specified maximum dose (**7**).
- Limit Dose (Gy) – defines the highest acceptable dose to any part of the OAR volume (**8**).

For both target and OAR volumes a weight (0-1000) need to be specified. This factor indicates the relative weight for the constraints of a structure, compared to the constraints of the other structures. To provide comparable contribution from both targets and OARs to the objective function, the OAR weights need to be lower than the target weights, this to compensate for the larger dose variance in OARs. It should be noted that hard constraints are not supported, i.e. no constraints are bound to be followed, but can be violated in a compromise solution.

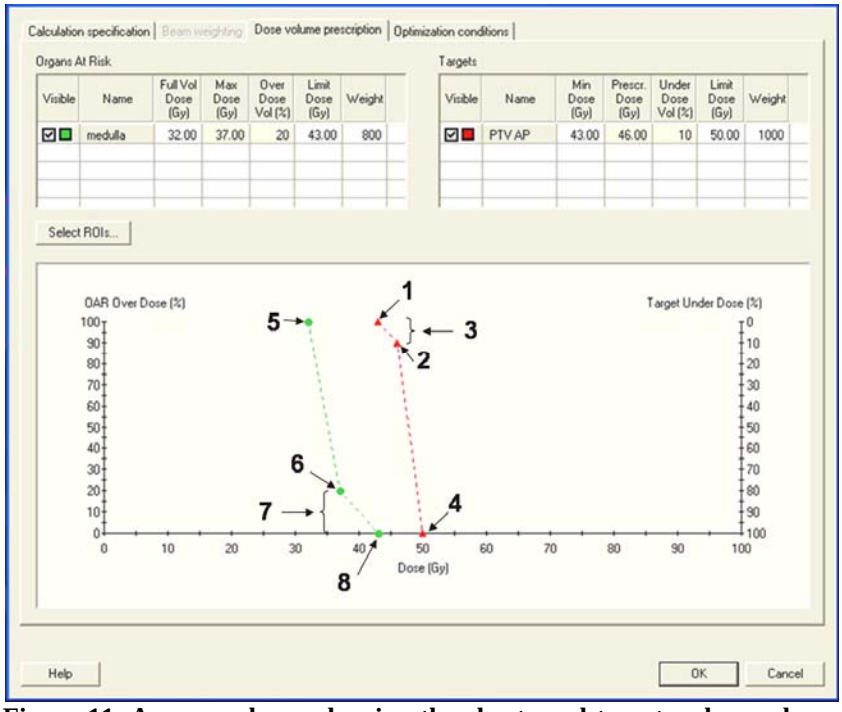

Figure 11. A screen dump showing the chart used to enter dose-volume constraints in the TPS.

3. The ARTSCAN Study

Many studies of head and neck carcinomas have shown that prolongation of overall treatment time has a negative impact on local control (Hansen et al. 1997). It is therefore of great interest to investigate whether a shortening of the overall treatment time will improve local control. It has already been shown that accelerated, hyperfractionated radiotherapy improves loco-regional control in head and neck squamous cell carcinomas but sometimes at the expense of increased late severe functional irradiation damage, such as myelitis (Horiot et al, 1997). ARTSCAN (Accelerated RadioTherapy of Squamous cell Carcinoma in the head And Neck) is an ongoing Swedish randomized controlled study. The aim of the study is to compare radical fractionated radiotherapy with accelerated fractionation with respect to local control, survival, quality of life and morbidity. Eligible for the study are patients with squamous cell carcinomas of all grades and stages in the oral cavity, larynx, hypopharynx and oropharynx (except smaller glottic carcinoma).

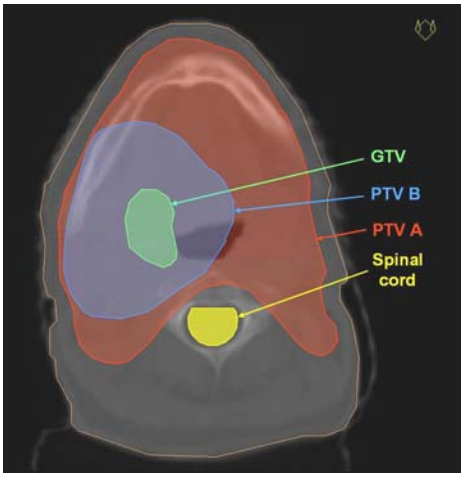

Figure 12. The different volumes that should be delineated according to the ARTSCAN protocol displayed in a tranversal cross section at the level of the mandible.

Various volumes are to be delineated according to the protocol (see Figure 12). The gross tumour volume (GTV) and planning target volume (PTV) should both be defined according to ICRU 50 (ICRU 1993), i.e. “the GTV is the gross palpable or visible/demonstrable extent and location of malignant growth” and consists of the primary tumour. The PTV contains, except the GTV, also subclinical microscopic malignant disease and margins for all possible geometrical variations such as set-up errors and organ movement. The protocol states that two PTVs should be delineated, PTV-A and PTV-B. Volume A must include volume B and should also contain estimated subclinical extensions at a distance. The size of these extensions might differ since it

depends on the traditions of treatment at each clinic. The first uninvolved lymph node station must however always be included in PTV-A. PTV-B (also called the boost volume) should consist of GTV, local estimated subclinical extension and all existing involved lymph nodes. Between GTV and PTV-B there should be a 20 mm margin when possible.

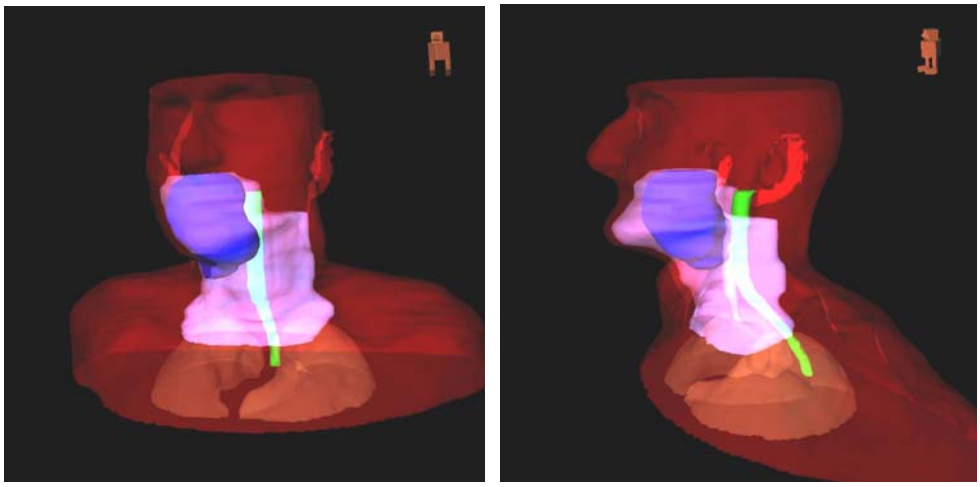

Figure 13. 3D views of the PTV-A (pink) including PTV-B (blue). The spinal cord is also shown in green.

In addition, the spinal cord should be delineated as an organ at risk (OAR). This is the only OAR that is mandatory to outline according to the present protocol. Recently, however, it was decided by the ARTSCAN group to consider several other OARs. The following organs will in the future also be delineated: parotid glands (both ipsi- and contralateral), the oral cavity, the submandibular glands, the mandible, the larynx and the upper part of oesophagus (see Figure 14). By delineating all of these OARs it will hopefully be possible in the future to correlate dose-volume data with acute and late side-effects.

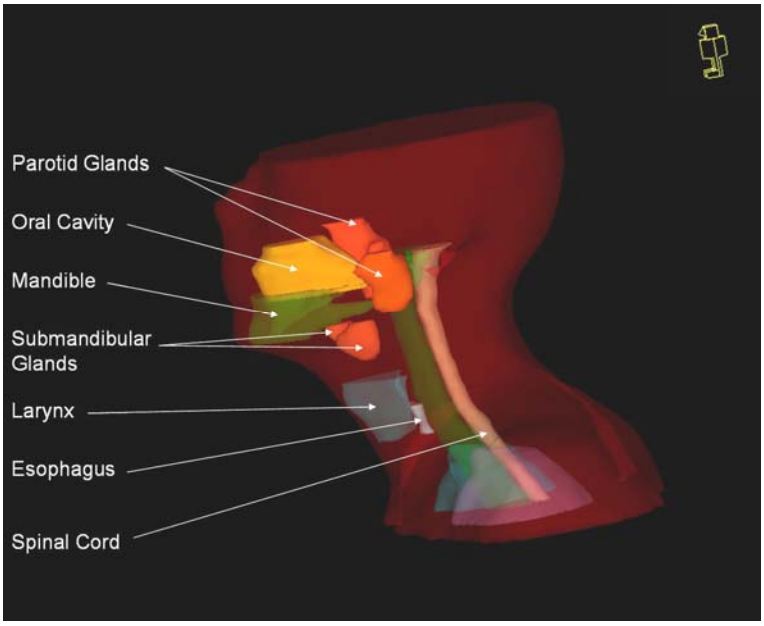

Figure 14. The organs at risk that will be outlined in the future in the ARTSCAN study.

The study consists of two arms, one control group receiving conventional radiotherapy and one experimental arm being treated with a concomitant boost technique. The patients in the control group are given 46 Gy in 23 fractions to PTV-A and then another 22 Gy in 11 fractions to PTV-B, leading to a total dose of 68 Gy. The treatment is given once a day, five days a week, resulting in an overall treatment time of 6.5 – 7 weeks. The experimental arm is receiving 46 Gy in 23 fractions to PTV-A and 22 Gy in 20 fractions to PTV-B, also leading to a total dose of 68 Gy. This arm is, however, given with a concomitant boost technique, i.e. for 20 days the patients are treated with two fractions per day resulting in an overall treatment time of 4.5 weeks. Fractions of 1.1 Gy are given in the morning to the primary tumour only (PTV-B) and then 2 Gy fractions in the afternoon to PTV-A. This ensures full repair of sublethal damage induced in the normal tissues when treating the large PTV-A as the time between the afternoon and morning fraction is usually more than 15 hours. The time interval between the morning fraction (PTV-B) and the afternoon fraction (PTV-A) should be at least 7 hours according to the protocol.

The total spinal cord dose should be kept as low as possible in all cases. The maximum total dose to the spinal cord must never exceed 48 Gy in any of the two treatment arms, with a maximum daily allowed dose of 2.1 Gy. The protocol also states that the volume of cartilage in the treatment field should be kept to a minimum since the sensitivity of cartilage to accelerated radiotherapy is yet not well known. No other organs at risk are discussed in the protocol, but as mentioned above, the ARTSCAN group has recently decided to consider supplementary organs at risk. However, no dose or dose-volume constraints on these organs have yet been specified.

4. Material and Methods

4.1 Experimental Equipment

The Oncentra Treatment Planning (OTP) system (version 1.2) from Nucletron has been used for the inverse planning of the patient cases. This system is not yet implemented in a clinical setting at our department. Hence, after optimization the plan was exported using the DICOM-RT protocol to our clinical TPS; Helax-TMS ver 6.1A, SP 1 (Nucletron). This TPS was only used for the final forward calculations. The recalculated plan was subsequently exported to our patient treatment verification system, Oncentra-Visir (Nucletron). The treatment unit was an Elekta SL*i* linear accelerator with beam qualities of 6 MV and 10 MV. The TPS, as well as the accelerator, only supports the step-and-shoot IMRT technique. The MLC replaces the upper jaws in the accelerator head (see Figure 15). It consists of 40 leaf pairs, all with a projected leaf width of 10 mm at the isocenter level.

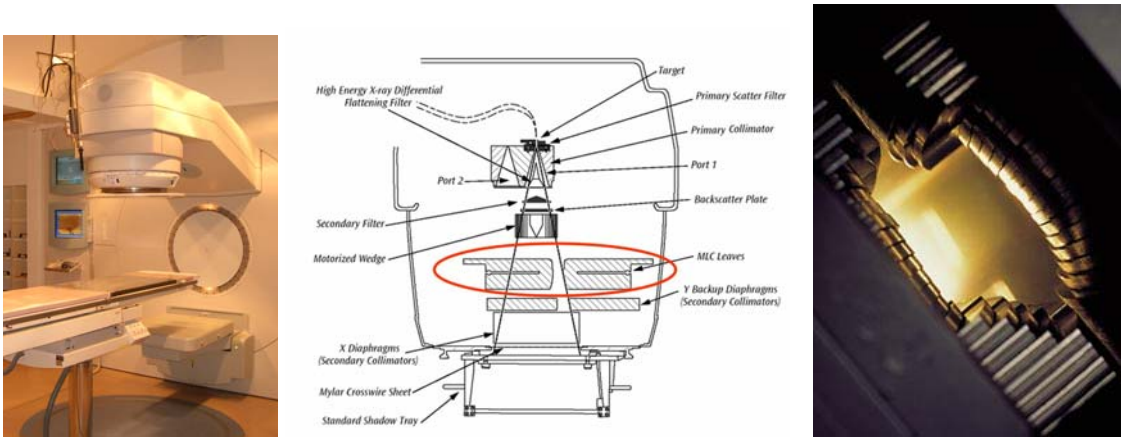

Figure 15. The accelerator (left) used for this study with an integrated MLC replacing the upper jaw system (middle). The right panel shows the leafs of the MLC from beneath.

4.2 Patient Characteristics

A total of five patients have been used for this treatment planning study. They were all diagnosed with squamous cell carcinoma of the tonsil with lymph node metastases. The five patient cases were considered to be typical for the majority of patients with this diagnosis included in the ARTSCAN trial. The five cases were selected by a radiation oncologist at the Radiation Therapy Department. The patients had all prior to this work received treatment according to the ARTSCAN protocol using conventional planning and treatment technique. Their age (at time of study randomization) and TNM classification are presented in Table 1.

Patient #	Age (years)	TNM classification
1	54	T2 N2 M0
2	52	T2 N1 M0
3	61	T3 N2a M0
4	39	T2 N2 M0
5	54	T1 N3 M0

Table 1. Patient demographics for the five studied patients.

Representative CT-scans with outlined targets for the patients are shown in Figure 16.

a) Patient #1

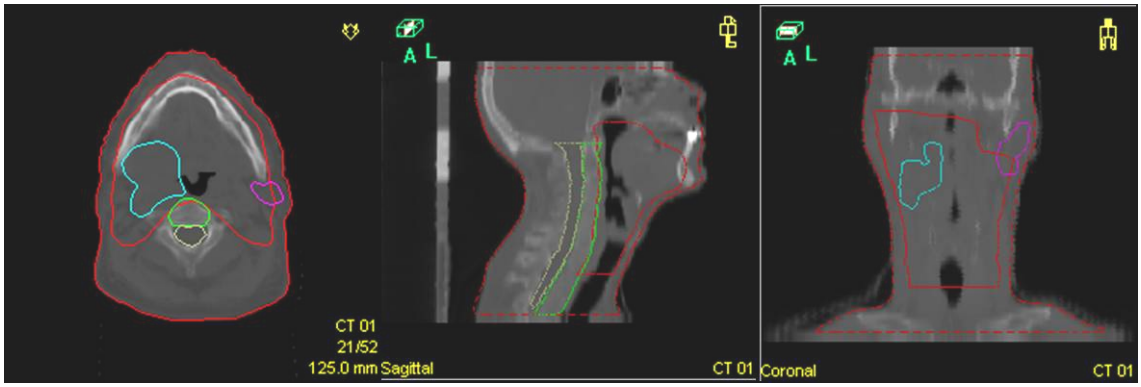

b) Patient #2

c) Patient #3

d) Patient #4

e) Patient #5

Figure 16. Representative CT-scans in transversal (left), sagittal (middle) and coronal (right) views of the five patients used for the treatment planning study. The light blue volume is the GTV. The larger red volume is the PTV-A and the smaller volume is PTV-B. The contralateral parotid gland is delineated in purple and the beige volume is the spinal cord.

4.3 Experimental Design

The influence of different treatment planning parameters (gantry angle, collimator angle, number of fields, number of intensity levels and segments per beam) on the dose distribution was investigated using mainly one randomly chosen patient (denoted patient #3 in Figure 16c). These results were then tested on the other four patients. A total of more than 150 IMRT plans have been created during the study. The physical parameters have been evaluated separately. After evaluating the first parameter it was held fixed while testing the next parameter, and so on. Strictly, for each variable all other parameters should have been varied. This would, however, have generated an enormous matrix, thus testing all possible combinations was not a realistic alternative.

Optimization was performed only on PTV-A, which was to receive 46 Gy in 23 fractions according to the ARTSCAN protocol. The desired dose distribution in the target volume was set to be 95 – 105 % (100 % corresponds to 46 Gy), also according to the protocol. When evaluating the plans, the results were rescaled, converting the mean

dose in PTV-A to 46 Gy. PTV-B has not been used for optimization purposes in any case. It is presumed at this instant that the boost treatment will be given based on conventional treatment planning.

The resulting maximum dose to the spinal cord after a full course of treatment will be slightly different in all cases depending on the dose contribution from the boost treatment as originally planned with conventional technique. This dose contribution was within the range of 2 – 3 Gy, providing a general maximum dose limit of no more than 45 Gy in the optimized plans. The contralateral parotid mean dose was to be kept below 26 Gy.

One advantage with IMRT is the possibility of delivering different dose levels to different regions at the same time, e.g. a medium-dose level to the tissues at risk for subclinical tumour spread, and a high-dose level to tumour-bearing tissues. This is normally referred to as simultaneously integrated boost (SIB). Many studies have shown that this technique results in treatment plans with a higher conformity and a reduced OAR dose (Bäck 2003, Wu et al. 2000, Mohan et al. 2000). The SIB technique will, however, not be considered in this work since the ARTSCAN protocol does not allow that as an option.

Before implementing a new method in the clinic it is of course important to be able to verify the treatment plans. Verification of our treatment plans has not been considered in this work, but is explored in a parallel study (La 2004).

4.4 Delineation of volumes

Since all patients were already included in the ARTSCAN study, the necessary volumes of interest were already delineated. However, PTV-A has in all cases been modified to be located not closer than about 10 mm from the skin surface to avoid overlap with the build-up region. In four cases a non-clinical volume equal to PTV-A plus a margin of 5 mm in all directions was used during optimization to avoid underdosage in the outer vicinities of the PTV-A. For the fifth case, adding a margin was not necessary to achieve a clinically acceptable plan.

Figure 17. The red volume is the modified PTV-A considering that the distance to the outline of the patient should not be less than 10 mm, whereas the green line shows the volume with an additional 5 mm margin. The OARs are delineated in yellow.

To avoid underdosage of the target volume, the contralateral parotid gland was delineated without any margins. Strictly, this is in contradiction to the recommendations of the ICRU (see above). The parotid gland is, however, a parallelly organized organ, and thus not critically sensitive to high doses in small parts of the organ. Under these circumstances and due to its close vicinity to the target volume it seems reasonable to omit the margin for such organs. This procedure has also been approved by the ARTSCAN group.

The parotid gland was partly located inside PTV-A in four of the patient cases. The part outside the target volume was delineated as a new VOI, used only for planning optimization purposes. This VOI has no biological meaning but helps avoiding underdosage in the junction between the target and the parotid gland. The spinal cord was already delineated with appropriate margins and there was no overlap of this organ at risk volume and the target volume in any case. There were no other critical structures defined in accordance with the study protocol.

4.5 Beam set-up (gantry, collimator angles and initial field shape)

The number of beams was varied from three to 13. To avoid parallel-opposed beams only odd number of fields within this interval was used. Both equiangular and non-equiangular beam arrangement set-ups were tested. Only coplanar beams were applied. It has been shown previously that the choice of collimator angles is not a critical parameter (Samuelsson & Johansson, 2003) and therefore this parameter has not been studied in the present work. To minimize the tongue and groove effect it has been suggested to use

slightly different collimator angles to avoid that the MLC leaves are exactly parallel for the different beams. We have, however, used a fixed collimator angle of 0° in all cases.

The user can specify the resolution of the dose calculation grid. If nothing else is stated a dose calculation grid of 3 mm has been used for the plans in this work. It was not possible to use a finer grid since this resulted in a failure during the optimization procedure. Some more complex beam set-ups, e.g. using 13 beams, required an even sparser grid (4 mm) to receive a result. The reason for this is unknown.

The user can specify the initial field shape. When applying the automatic MLC tool in the TPS, the user must specify how to set the leaves. The user can choose to let the leaves follow either the collimator or one of the structures (with or without applying a margin) when shaping the field. The initial field shape is of no importance, since the modulation segmentation does not take any user-specified field size into account, nor does it consider the initial MLC settings. It is recommended, however, to use the collimator to set the leaves. When not doing so, sub-beams violating the MLC-constraints are sometimes generated, resulting in a non-usable plan.

4.6 Total Number of MLC Segments

After determining the optimum number of fields there are two different methods to affect the total number of MLC segments in the plan, i.e. changing the number of levels in the intensity map and setting an upper limit for the number of segments in each beam. These two parameters are obviously related but have in this work been evaluated separately.

Five different intensity levels (2, 5, 7, 10 and 15) were tested. After choosing a sufficient/optimal number of intensity levels, the number of segments per beam was evaluated. Six plans were optimized, all with a different number of maximum segments allowed (3, 5, 7, 10, 15 and 20).

4.7 Photon Beam Quality and Treatment Unit

The beam quality mainly used in this work has been 6 MV. Two other energies (4 and 10 MV) were also tested. All other parameters were identical and the plans were optimized using the three beam qualities on the same treatment unit (L03[3]).

Optimization was performed on three different clinical treatment units (L03, L10 and L22[3]) in our clinic and also on a demo version of a Siemens Primus accelerator present in the TPS to check the dependency on different MLC systems. To further verify the MLC influence on the dose distribution, a modified Elekta accelerator with no MLC constraints (all leafs can be positioned freely) was installed in the treatment unit database of the TPS. The modulation matrices before segmentation were compared to the discretized intensity maps that actually would be delivered.

---

[3] L03: Elekta Precise with 4, 6 and 10 MV

L10: Elekta SL*i* with 6 and 10 MV

L22: Elekta SL*i* plus with 6 and 18 MV

4.8 Dose-volume Constraints and Weight Factors

Determination of optimal dose-volume constraints and weight factors is a trial and error process. When all other parameters have been optimized the dose-volume constraints and weight factors have to be modified until a clinically acceptable dose plan is achieved. Dose-volume constraints for the target volume have been set to follow the prescribed dose; however, the maximum and minimum doses are preferably set to somewhat stricter values than actually aimed at to optimize the PTV coverage. The constraints for the OARs, however, must usually be set to a lower dose than actually accepted to assure that tolerance doses are not exceeded. After finding a clinically acceptable plan, the weight factors of both the target volume and OARs were changed slightly (independently) to evaluate their influence on the dose distribution.

4.9 Evaluation of Treatment Plans

The treatment plans were evaluated with physical parameters such as the dose-volume histograms (DVH) and the fraction of the PTV receiving at least 95 % of the prescribed tumour dose (PTV95). The minimum and maximum doses to the PTV were also recorded. These doses/volumes, however, should be clinically relevant. The minimum dose reported should not be located in the build-up region and the maximum dose reported should be within a contiguous volume with a diameter exceeding 15 mm. A homogeneous dose to the PTV was strived for. The homogeneity is normally evaluated using the standard deviation around the mean dose. OTP, however, currently does not calculate this figure and thus the standard deviation will only be reported for the plans exported to and forward calculated in the Helax-TMS. For the OARs, the maximum dose to the spinal cord and the mean dose to the contralateral parotid gland were evaluated. Plans exceeding the tolerable doses (45 and 26 Gy, respectively) for the OARs were rejected.

4.10 Inter-hospital comparison of optimized treatment plans

The optimal plans produced were compared with plans generated (on the same patient) at the Departments of Radiation Physics at Umeå University Hospital and at Sahlgrenska University Hospital in Göteborg. Umeå has the same treatment planning equipment as used in this work and this comparison, therefore, shows an example of variation between different treatment planners. It should be noted, however, that they modified the planning target volume according to traditions at their clinic. Göteborg has equipment (treatment planning system and accelerators) from Varian Medical Systems. The plan was here optimized using the dynamic MLC technique. By comparing this plan with our own, we get a test mainly on the equipment performing the optimization.

5. Results and Discussion

5.1 Beam set-up (gantry, collimator angles and initial field shape)

The treatment plan was improved when the number of fields was increased, as shown by the improvement in PTV95 (Figure 18). This is in agreement with other studies (e.g. Wu et al, 2002). It has also been shown that beyond a certain number of fields the improvement becomes negligible, but this specific number of fields differs in the literature, ranging from three to nine (Stein et al, 1997, Söderström et al, 1995, Wu et al, 2000). This study shows a significant improvement up to seven beams. A further increase of the number of fields shows no or little improvement. The choice of seven beams as the optimal number is also to some extent chosen so that the treatment time per fraction becomes reasonable, as discussed below under total number of segments.

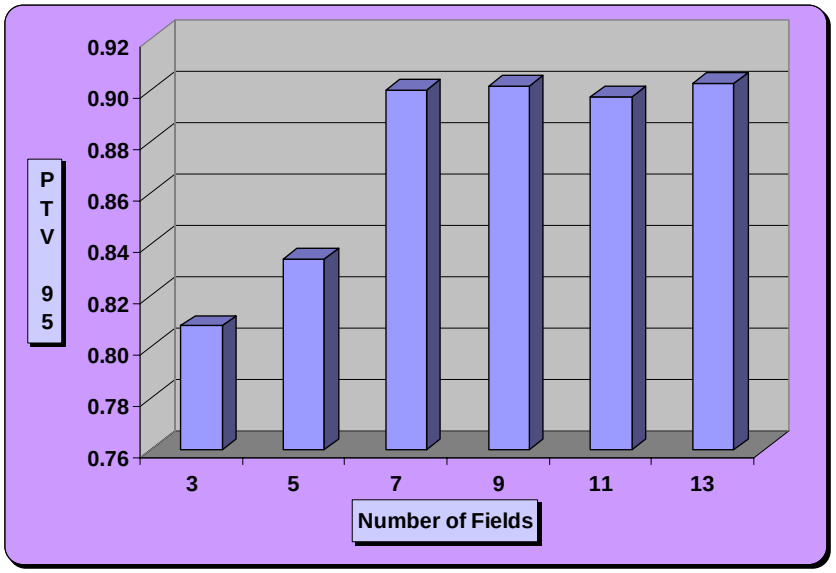

Figure 18. PTV95 for different number of fields.

A few optimizations with non-equiangular beam arrangement were performed (Figure 19). The beams were oriented as for conventional treatment planning and proposed by an experienced treatment planner at our department. It was also tested whether using beams, coming from the direction of sensitive structures (spinal cord and the parotid gland), would improve the plan. Directions like these were proposed by Stein et al, 1997, since according to this author, they would allow greater control over the dose distribution. In this study, the use of non-equiangular beam arrangement showed no clinically significant improvement. This is in agreement with other studies, where it has been shown that optimizing beam orientation only is valuable for five beams or less (Stein et al, 1997 and Söderström et al, 1995). Furthermore, Bortfeld and Schlegel (1993), showed that the

optimum beam configuration for multiple-beam irradiations with more than three beams tends to be an even distribution over an angular range of 0 to 360º.

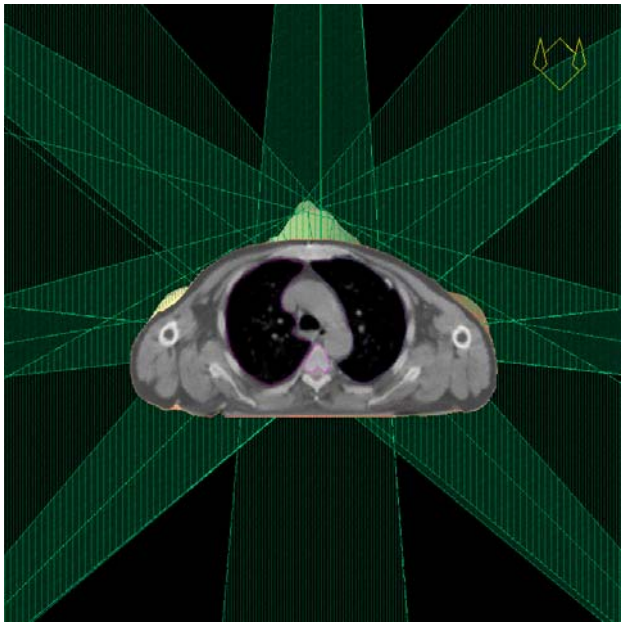

Figure 19. Example of beam directions for the non-equiangular beam arrangement case (gantry angles: 225°, 260°, 305°, 0°, 55°, 100° and 135°).

5.2 Total Number of MLC Segments

The delivery time for one fraction is in conventional radiotherapy usually around a few minutes. IMRT, especially with the step-and-shoot technique, will considerably prolong the delivery time. This is a disadvantage for several reasons, e.g. from a cost-efficiency point of view where the number of treated patients per day would have to be decreased as the treatment time is extended. Many patients are old and suffering from pain, thus having a hard time lying still during the treatment. Therefore, the prolonged treatment time would increase the risk of set-up errors. Furthermore, the effective dose rate, which will be lowered with prolonged delivery time, might have an effect on the biological effect on the tumour. It has been shown that prolonging the fraction time will spare tissues with a fast DNA repair (Mu et al, 2003), implying a risk of tumour sparing. For delivery times longer than 15 minutes, Wang et al. suggest an increase of the prescription dose to compensate for the reduction in cell killing due to the increased sublethal damage repair (Wang et al, 2003).

Although the delivery time could be lowered by e.g. using a magnetron with a faster response time or increasing the dose rate on the accelerator, it is strongly dependent on the total number of MLC segments. This is due to the relatively slow movement of the MLC leaves during the "radiation-off" period when changing position to create a new sub-field in the sequence. This study shows that 10 intensity levels are sufficient (Figure 20). Using this result while evaluating the number of segments allowed per beam shows

no significant improvement for more than 10 segments per beam (Figure 21). With seven beams and a maximum of 10 segments per beam, the total number of segments would be 70. In practice, however, the total number of segments for this arrangement is rarely above 60. Keeping the number of segments below 60 is advisable since it implies a treatment time of less than 20 minutes per fraction using our equipment.

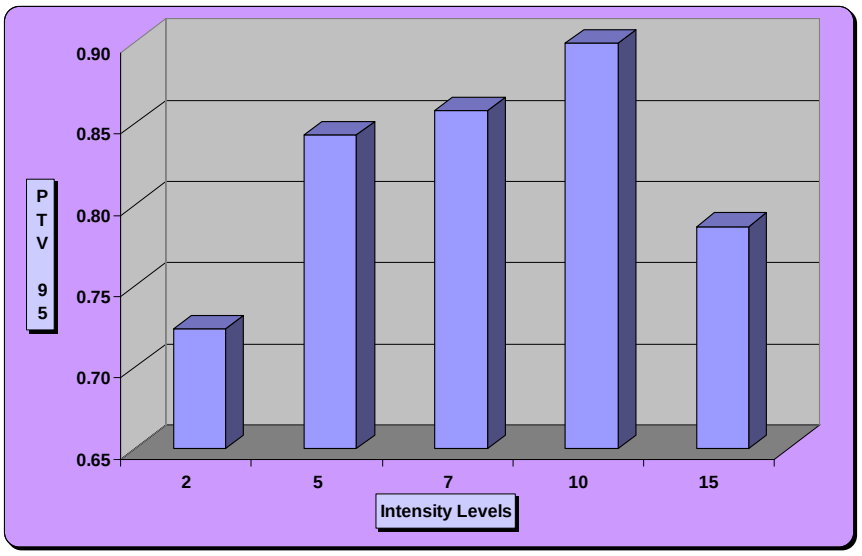

Figure 20. PTV95 for different number of intensity levels.

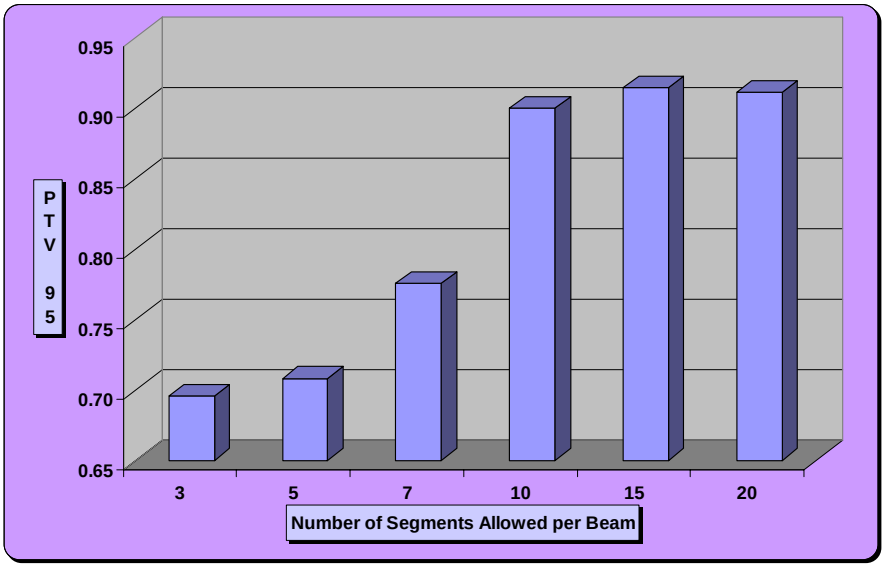

Figure 21. PTV95 for different number of maximum segments per beam.

5.3 Photon Beam Quality and Treatment Units

Plans optimized with different beam qualities showed similar results and the differences were hardly clinically significant. This is in agreement with Söderström et al, 1999, where it is shown that the use of optimized intensity modulated photon beams significantly reduces the need of beam energy selection. The same study also suggests that regions with organs at risk located laterally close to the target volume, which is the case for the patients used in this study, would benefit most from using low photon energies due to their smaller penumbra. Since the 4 MV quality is not so frequently existing, 6 MV is chosen to be the most suitable beam quality for IMRT in this patient group.

We did not expect any clinically significant differences in the IMRT plan quality when optimizing on the different Elekta accelerators available. It is, however, likely that the Siemens accelerator would generate differences in the optimized treatment plan, since the MLC is different, and more importantly, the MLC constraints are different. Using the Siemens Primus Demo Version resulted in a somewhat different plan, but with no obvious clinically significant improvement. Since the results obtained so far was not as good as expected a comparison between the modulation matrix before segmentation and the intensity map used for delivery was performed. The matrices were quite different (see Figure 22), implying that the modulation segmentation is not optimal. The cause of this could possibly be the way the MLC constraints are handled. After discretizing the modulation matrix, the sub-beams that would best imitate the matrix are generated. The sub-beams violating the MLC constraints are then simply omitted. Depending on the importance of these invalid segments, this process could significantly change the final result.

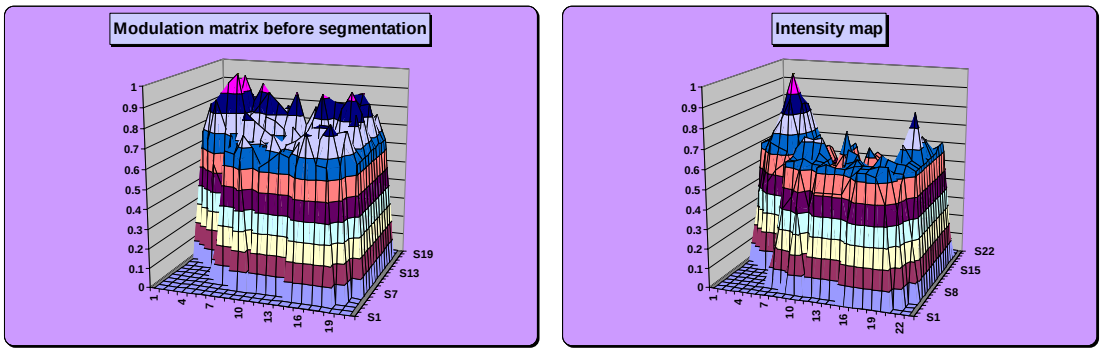

Figure 22. Comparison of the modulation matrix before segmentation (left) and the actual TPS intensity map (right) for an Elekta SL*i* accelerator.

Thus, it is of interest to make the same comparison for an accelerator without any MLC constraints at all. From the results in Figure 23, it is obvious that the two matrices are in better accordance for this accelerator. This optimized plan was also clinically superior.

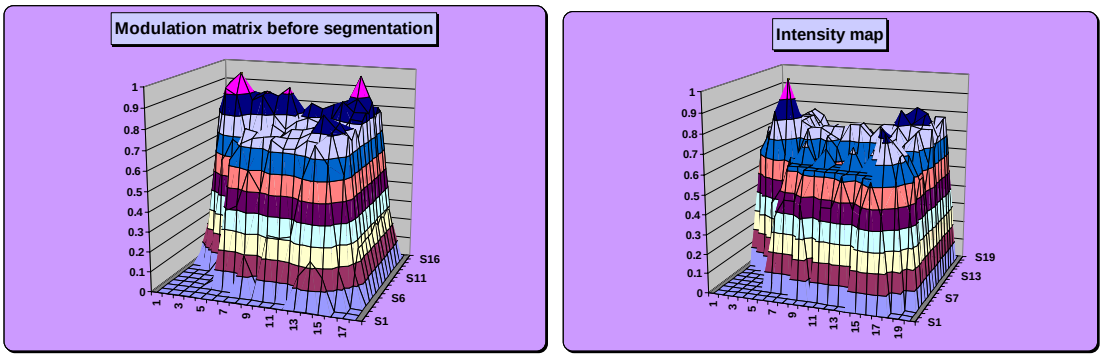

Figure 23. Comparison of the modulation matrix before segmentation (left) and the actual TPS intensity map (right) for an Elekta SL*i* accelerator where the MLC-constraints have been removed.

5.4 Dose-volume Constraints and Weight Factors

It was found that the optimal dose-volume constraints for the minimum and maximum dose in the PTV should preferably be set somewhat tighter than the dose range of 95-105 % stated in the ARTSCAN protocol. The prescription dose is 46 Gy and assigning the minimum dose to 45.5 Gy (≈ 99 %) and the limit dose to 47 Gy (≈ 102 %) helps achieving the 95-105 % coverage goal. The goal of covering the whole target volume with the 95 % isodoses curve was never accomplished for any of the patients. It should be noted, however, that 95 % coverage was not achieved in the existing conventional plans either.

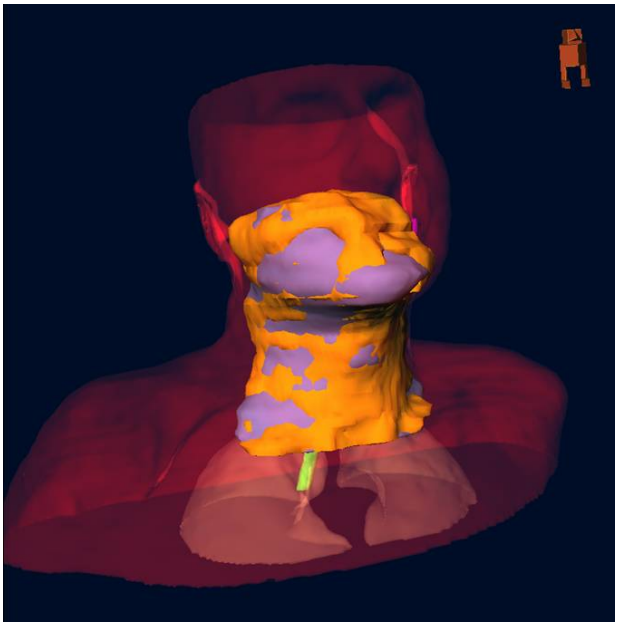

Figure 24. PTV-A (blue) is not completely covered by the 95% isodose surface (orange).

The dose-volume constraints for the OARs must also be set to achieve clinical acceptance. For the spinal cord, assigning a maximum dose of 37 Gy, a full volume dose of 32 Gy, a limit dose of 43 Gy and allowing an overdosage volume of 10 % would in general generate a maximum absorbed dose of less than 45 Gy. For the parotid gland the optimal dose-volume constraints was found to differ quite substantially between different patients since the constraints are assigned to the part of the gland that does not overlap the PTV. The dose-volume constraints will therefore obviously be dependent on the relative size of this joint volume. Thus several modifications of the constraints had to be performed to keep the mean dose below 26 Gy. For the majority of the patients in this work, the full volume dose was assigned to 15 Gy, the maximum dose to 20 Gy, the limit dose to 25 Gy and allowing an overdosage volume of 25 %.

The influence of different weight factors was initially tested by trial and error. A good result was obtained with the values 1000, 650 and 300 for the PTV, the spinal cord and the parotid gland, respectively. To further analyze the influence of the weight factors, tests were performed with weight factor settings close to these values. In Figure 25, seven plans with weight factors according to Table 2, are presented. Plan number one is the reference plan. In number two and three the spinal cord weight has been changed, whereas the parotid gland weight has been modified in plan number four and five. No significant improvement can be seen. In plan number six and seven the PTV weight factor has been decreased. The poor result is quite obvious. A weight factor of 1000, i.e. maximum weight, is therefore recommended for the PTV.

Plan #	PTV-A	Spinal Cord	Parotid Gland
1	1000	650	300
2	1000	500	300
3	1000	800	300
4	1000	650	200
5	1000	650	400
6	850	650	300
7	700	650	300

Table 2. The weight factors for PTV-A, the spinal cord and the parotid gland in the different plans presented in Figure 25 below.

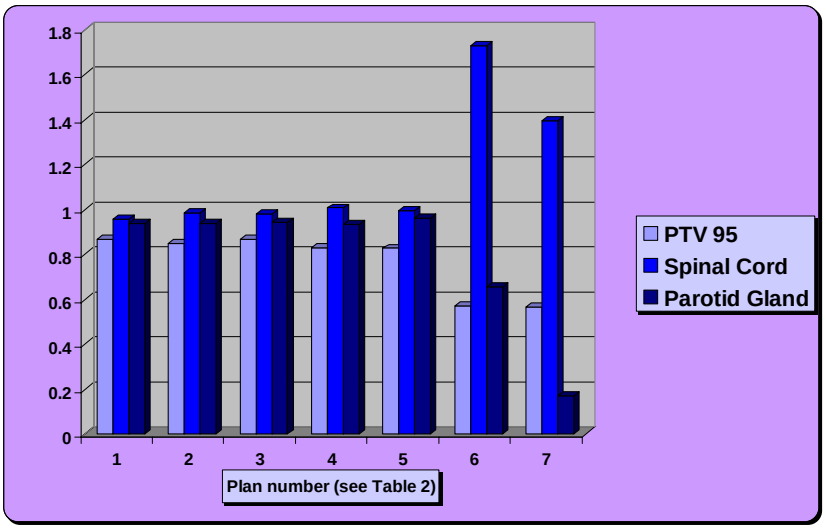

Figure 25. The influence of different weight factor settings is shown (see Table 2 for the exact weight factors applied). The presented OAR doses are the maximum dose for the spinal cord, normalized to 45 Gy, and the mean dose for the parotid gland, normalized to 26 Gy.

5.5 Influence of PTV delineation and patient geometry

With the optimization algorithm used it is often quite difficult to obtain proper dose coverage in the peripheral parts of the target volume. This problem could in general be solved by adding a 5 mm margin to the PTV for planning purposes only. There are efficient tools to perform this automatically in the TPS image registration and structure definition modules. This process is thus not time consuming. In some cases, however, a 5 mm margin is not enough, but would have to be increased in some of the CT slices. Adding a larger margin to the entire volume would give rise to an unnecessary normal tissue dose to the patient. Manually modifying the margin in selected CT slices was found to be an unrealistic approach. This process easily becomes very time consuming since modifying the margin volume at one specific location to improve target coverage here, often lead to a decrease in coverage at some other location in the target volume.

The head and neck geometry is very complex and varies from patient to patient, "stressing" the optimization algorithm. Even seemingly small inter-patient variations could sometimes result in none or bad convergence of the objective function leading to clinically unacceptable treatment plans. In these cases, the system does not present any error messages but the log files display a failure in the line search with the consequence that the objective function is not updated between the iterations. The optimization is thus ended since the termination criteria of the objective function fractional changes are being fulfilled. This problem, where the optimization gets trapped in solutions from where it cannot escape, seems to be random. This will obviously be a problem when implementing IMRT in the clinic, when one would want to be certain that it is possible to find an acceptable plan for all individuals within the selected patient group. There are no recommendations from the vendor to remedy this problem. By changing different

parameters such as VOI geometry, weight factors and/or dose-volume constraints, the optimizations were finally succeeded for all patients in this study. This is however a time consuming method with an uncertain outcome. It is therefore our opinion that the IMRT module in the used TPS has to be improved considerably and that it is currently not well suited for clinical routine use.

5.6 Comparison with Existing Conventional Plans

Comparisons of the optimized IMRT plans with the existing conventional plans actually used for treating the patient are presented in Table 3. For patients 1-4 the conventional plans show better dose coverage (PTV95) and smaller standard deviation, but will most probably lead to permanent xerostomia for the patients, since the parotid mean absorbed dose is above 26 Gy. For the IMRT plans, the parotid mean dose is well below 26 Gy and the dose to the spinal cord is also somewhat lower compared to the conventional plans. For patient number five, however, an attempt of parotid sparing using conventional technique was made. It is clear that the IMRT plan in an overall sense is superior in this case.

	Patient #1		*Patient #2*		*Patient #3*		*Patient #4*		*Patient #5*	
	IMRT	**Conv.**	**IMRT**	**Conv.**	**IMRT**	**Conv.**	**IMRT**	**Conv.**	**IMRT**	**Conv.**
Max. PTV (%)	112	108	111	108	115	110	108	107	110	127
Min. PTV (%)	70	83	73	91	80	88	69	88	87	16
Std.dev. (%)	4.5	2.6	3.5	2.8	3.7	2.7	3.3	3.0	2.9	12.3
PTV95 (%)	93	98	96	99	95	98	95	98	98	94
Sp. cord (Gy)	42.9	45.9	42.6	44.7	42.7	45.9	40.1	45.8	42.2	46.8
Parotis (Gy)	22.9	27.3	25.3	31.8	24.1	30.1	24.3	27.6	21.9	20.5

Table 3. Comparison of the IMRT plans and the conventional plans for the five patients. The presented OAR doses are the maximum doses for the spinal cord and the mean doses for the parotid gland.

In Figures 26-28 the 3D dose distribution for the conventional plan of patient #3 is compared to the IMRT plan. To produce the 3D pictures for the conventional case (planned in Helax-TMS), the treatment plan had to be reconstructed in OTP. The patient was originally treated on a Varian Clinac accelerator using enhanced dynamic wedges. Dynamic wedges are currently not supported by OTP; hence the presented plan is reconstructed using fixed wedges. The PTV-A has also been modified in the build-up region as described above. However, the final result is very similar to the treatment plan the patient was actually treated with. In Figure 26 the orange surface is the 95 % isodose surface and the blue volume is the PTV-A. The problem with the PTV coverage in the IMRT plan is nicely illustrated. Figures 27 and 28 show the benefit of IMRT concerning normal tissue sparing for the parotid gland and the spinal cord, respectively.

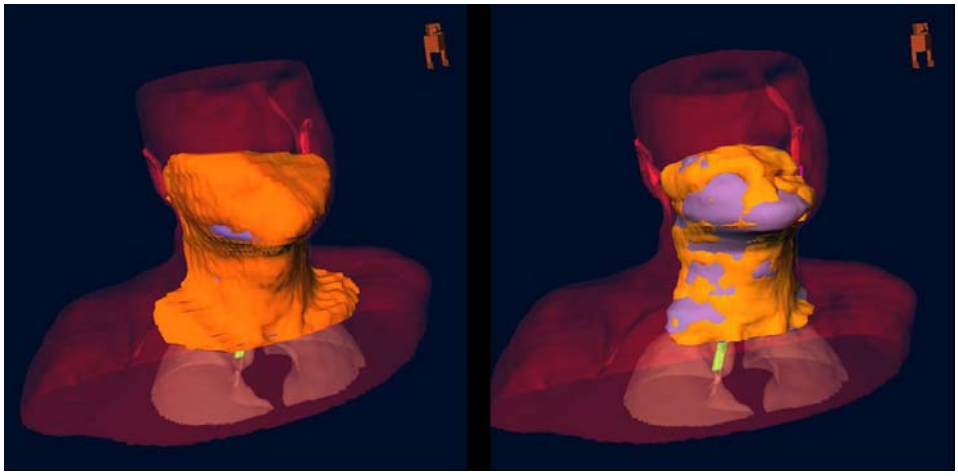

Figure 26. The 95 % isodose surface (orange) for the conventional plan (left) compared to the IMRT plan (right).

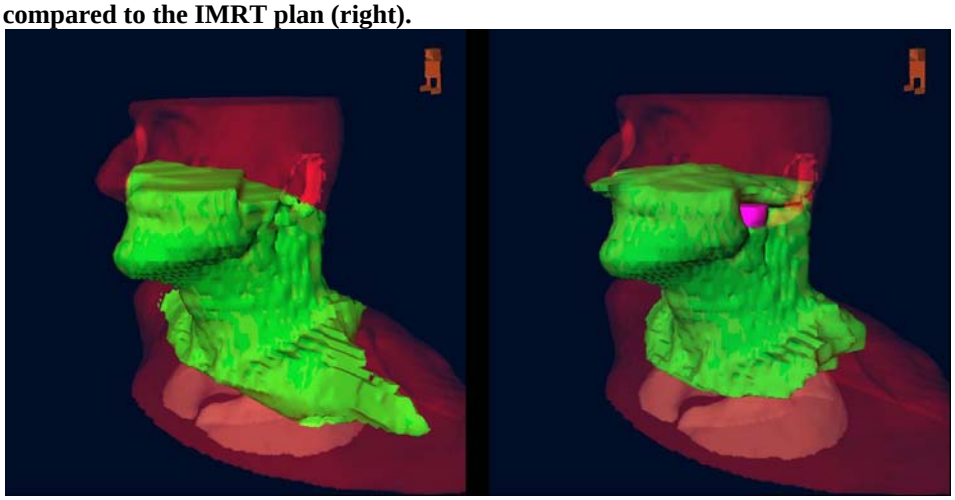

Figure 27. The green volume is the 15 Gy isodose surface for the conventional plan (left) and the IMRT plan (right). The purple volume in the IMRT plan is the contralateral parotid gland, which, in the conventional plan, is completely covered by the 15 Gy isodose surface.

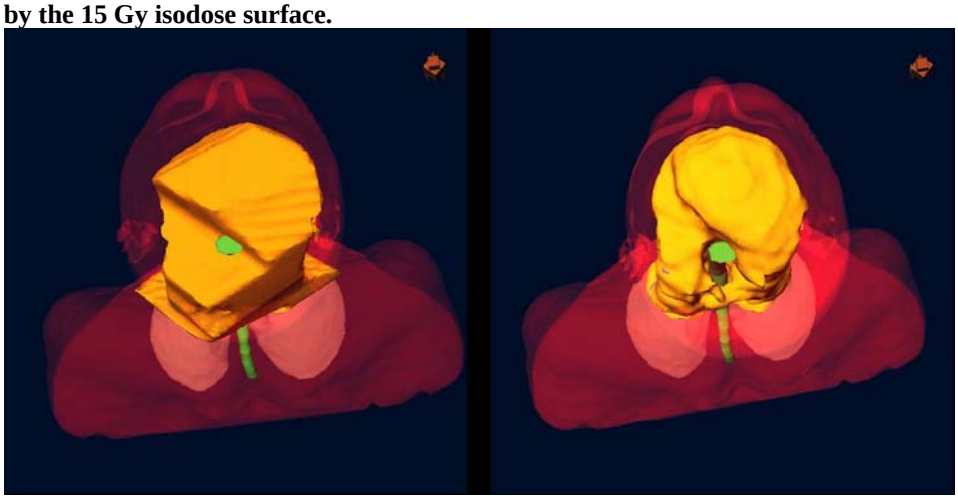

Figure 28. The orange volume is the 40 Gy isodose surface as seen from above for the conventional plan (left) compared to the IMRT plan (right).

In Figure 29 the dose-volume histograms for the PTV-A, the spinal cord, the parotid gland and the total body are presented for patient #3. The DVH for the PTV-A shows just barely a better PTV coverage in the conventional plan (blue line). For the spinal cord and the parotid gland, on the other hand, it is quite obvious that the IMRT plan (purple line) is superior. It should also be noted that the there is no significant difference in the total body dose, which might be expected. The DVHs for the other patients show very similar results.

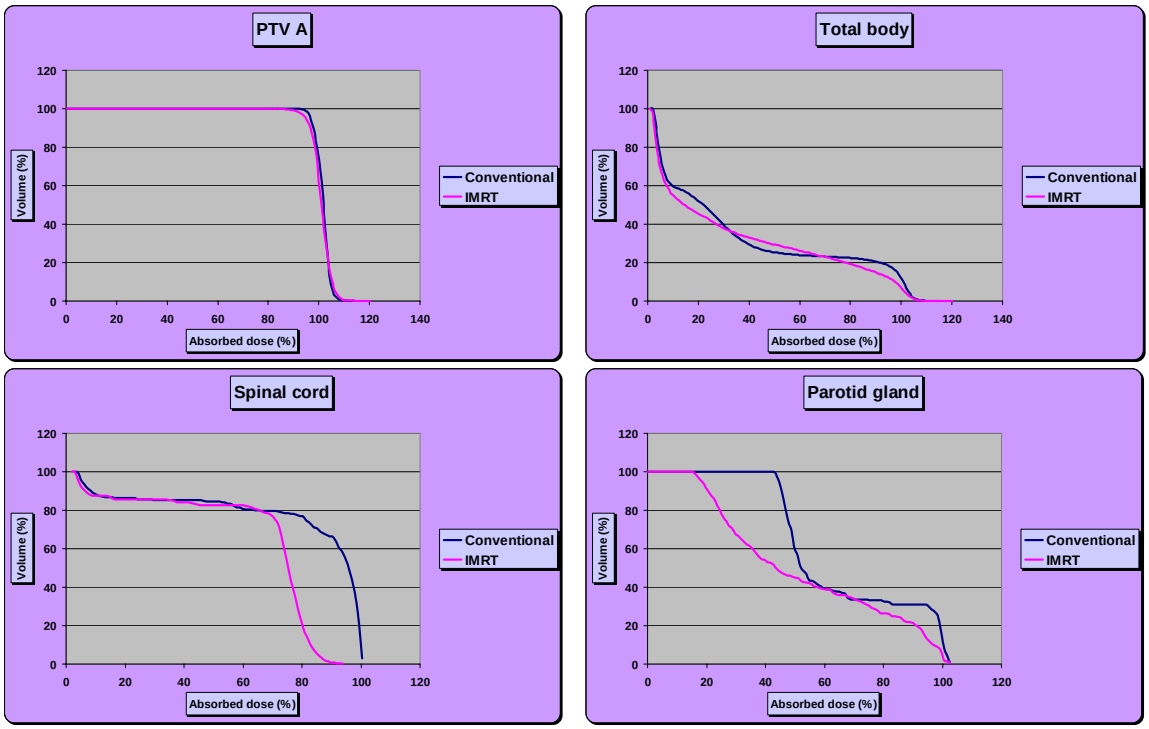

Figure 29. DVH comparisons of the IMRT plan (purple) and the conventional plan (blue) for patient #3.

Before implementing IMRT in the clinic, it has to be shown clearly that the optimized plan is better than the existing one. There are several factors to consider when deciding whether this is the case, e.g. target coverage vs. normal tissue sparing. In this work we found that the mean dose to the parotid gland could be kept below 26 Gy, however with a slightly worse target coverage compared to that obtained with conventional treatment planning. It is of course of importance that the normal tissue sparing shown in this work actually leads to the expected result, i.e. a time-related recovery of the acute xerostomia. Since the biological effect on the parotid gland is dependent on the mean dose, an anatomically correct delineation of this OAR and lack of organ movement becomes very important. Using a PRV (as proposed by Manning et al, 2001) would decrease the risk of exceeding the tolerance dose as a result of geometrical uncertainties. It should also be noted that only the mean dose of the major salivary glands has been considered in this work. To further reduce xerostomia the minor salivary glands in the oral cavity should

also be included in the planning objectives. These minor glands have been found to be a significant independent predictor of xerostomia, and the radiation effect can be represented by the oral cavity mean dose (Eisbruch et al, 2001). Since it has been decided that the oral cavity (amongst other structures) should be delineated as an organ at risk in the ARTSCAN study from now on, this can be used to further reduce permanent xerostomia in the future. It has also been proposed that other dosimetric parameters of the parotid glands, such as the maximum dose, correlates to subjective salivary gland function (Amosson et al, 2003), suggesting a more complex organ function than considered in this work.

The disadvantages of an IMRT treatment plan need also to be considered; the most obvious one probably being the inhomogeneous target dose. In all plans but one presented above, the standard deviation of the PTV mean dose is larger than for the existing conventional plans. A standard deviation of less than 3.5 % (Mijnheer et al, 1987) and 3 % (Brahme et al, 1988) has been proposed as a clinical goal. A larger standard deviation might lead to loss in tumour control probability. These figures are dependent on the expected biological response gradient and will thus vary with tumour type. It should be noted, though, that the majority of loco-regional recurrences after parotid-sparing segmental IMRT in the head-and-neck region have been reported to be located "in-field", i.e. parotid sparing might not compromise local control (Dawson et al, 2000). It is, however, yet not known if this conclusion could be generalized.

5.7 Inter-hospital comparison of optimized treatment plans

Representative CT slices from the plans optimized in Umeå (Figure 30) and in Göteborg (Figure 31) are shown compared to the same slices from the optimal plan produced in this work.

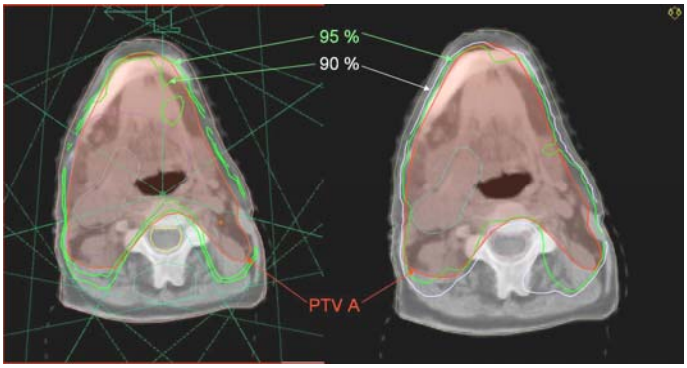

Figure 30. The plan optimized in Umeå (left) compared to our optimal plan (right).

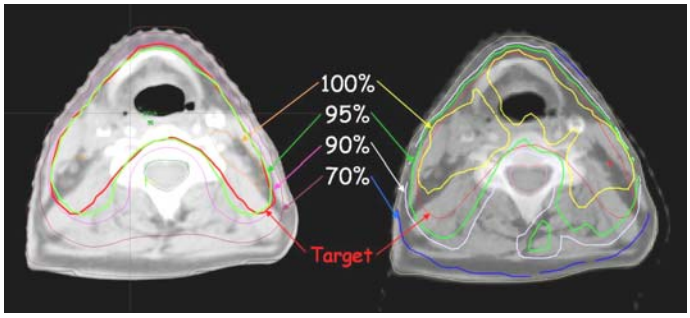

Figure 31. The Göteborg plan (left) compared to our plan (right).

The Umeå plan has been optimized using the same TPS as in this study. However, the target volume has been slightly modified according to their treatment traditions. This implies splitting the target at approximately two centimetres below the GTV. The caudal part of the target is then further divided into two parts located on each side of the oesophagus. By doing this, both oesophagus and the thyroid gland can be spared. IMRT is then only needed for the cranial part of PTV-A. The Umeå plan also contains an additional structure located dorsally of the spinal cord to help avoid high doses in this region. Furthermore, the treatment plan has been manually modified after the forward calculation in Helax-TMS to eliminate any existing hot spots and also to try to raise the minimum target dose. These modifications to the patient geometry and the treatment plan are consistent with the actual treatment methods used in the Umeå clinic. In Table 4 a summary of the three different plans is presented. The minimum PTV dose, as well as the normal tissue doses, is slightly better for the Umeå plan, but the PTV95 is on the other hand better for the Lund plan.

The treatment plan created by the group in Göteborg has been optimized using different equipment and delivering method (Eclipse TPS, Varian Medical Systems and dMLC technique). When comparing the 95 % isodose curves (green) in Figure 31, it is quite clear that the conformity is better in the plan from Göteborg. In Table 4 it is also shown that the normal tissues doses are lower for the Göteborg plan as well as the standard deviation in the mean PTV-A dose.

	Lund	*Umeå*	*Göteborg*
Max PTV-A dose (%)	115	113	104
Min PTV-A dose (%)	80	87	68
SD in PTV-A (%)	3.7	3.5	1.0
PTV95 (%)	95	91	95
Spinal cord max dose (Gy)	42.7	37.4	40.3
Parotid gland mean dose (Gy)	24.1	18.1	19.0

Table 4. Comparisons of the IMRT plans for patient #3 optimized at different hospitals.

The results are further illustrated with the DVHs in Figure 32. These results show that the quality of an IMRT plan is strongly dependent on the equipment used.

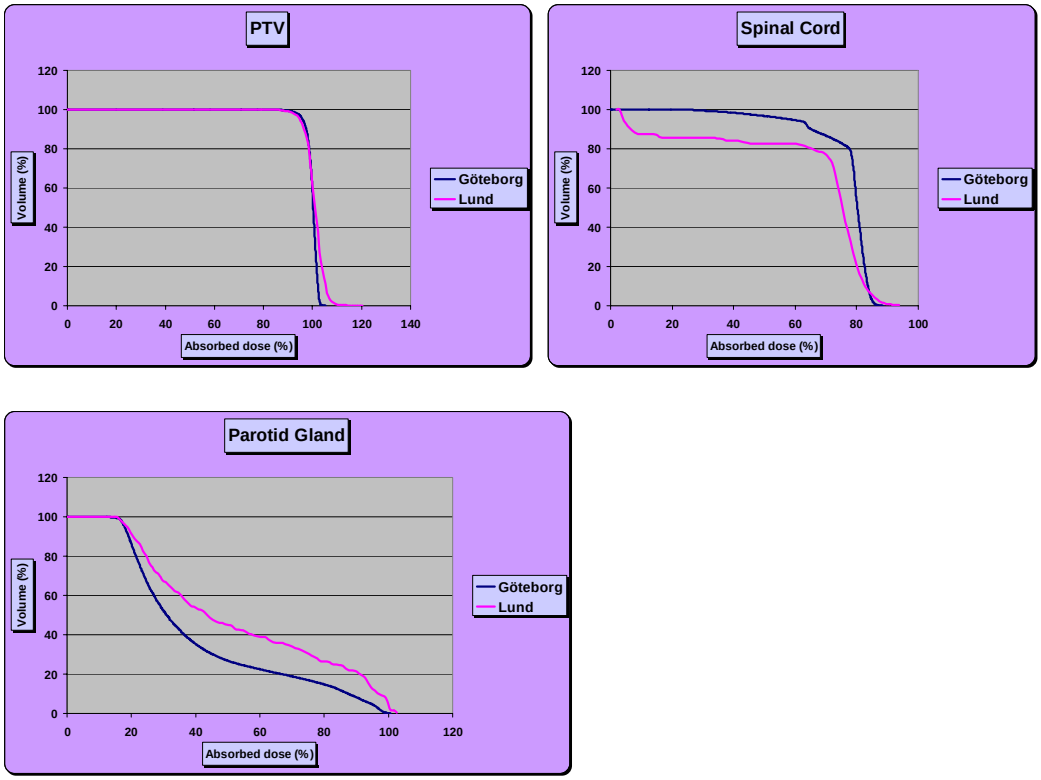

Figure 32. DVH comparisons of the IMRT plans from Göteborg (blue) and Lund (purple).

6. Conclusions

The purpose of this study was to investigate whether inversely planned IMRT, using the clinical radiotherapy equipment at hand in our department, renders any advantages regarding dose distribution over conventional radiotherapy for head and neck cancer patients in the ARTSCAN study, with special consideration to parotid sparing. The results in this work clearly show the benefit of IMRT concerning normal tissue sparing. The mean dose in the contralateral parotid gland is easily kept below the threshold dose of 26 Gy in the IMRT plans. The spinal cord maximum dose is also usually lower for the IMRT plans compared to the conventional plans. The normal tissue sparing is, however, always achieved at the cost of target coverage. This fact makes it complicated to decide whether the IMRT plans are clinically advantageous over the conventional plans. This work has also shown the influence of the equipment used. Comparison between our IMRT plan and an IMRT plan optimized using equipment from another vendor (both TPS and delivery system are different) clearly shows the fact that it is possible to create a better treatment plan, regarding both target coverage and normal tissue sparing, using IMRT.

7. Acknowledgements

I would like to express my genuine gratitude to my supervisors Per Nilsson and Tommy Knöös for encouragement, support and excellent guidance. Thanks to you, this past semester has been wonderful and memorable, and I am really glad I got the chance to work with you.

There have been many other persons who have been important for the completion of this work and whom I also would like to thank:

Lidia Karolak for all the help regarding TMS and for being so patient when my test patients filled up the disk and when the back-up did not start because of me,

Elisabeth Kjellén for medical guidance, help with choosing suitable patients and evaluating dose plans and for helping me better understand the complex anatomy of the head and neck region,

Karl-Axel Johansson at the Department of Radiation Physics at Sahlgrenska University Hospital in Göteborg for all help and for taking so good care of us during our visit to Göteborg, it was very interesting,

Magnus Karlsson and Rickard Sjögren at the Department of Radiation Physics at Umeå University Hospital for all the help and interesting mail correspondence,

Everyone at the department in Lund for all help and interesting discussions, you have all made my time here unforgettable.

I also really would like to thank Sonny La for stimulating collaboration and valuable discussions, and for all the help when I really needed it. You are a true friend.

References

1. Amosson C M, Teh B S, Van T J, Uy N, Huang E, Mai W-Y, Frolov A, Woo S Y, Grant III W H and Butler E B. *Dosimetric Predictors of Xerostomia for Head-and-Neck Cancer Patients Treated with the SMART (Simultaneous Modulated Accelerated Radiation Therapy) Boost Technique.* Int. J. Radiation Oncology Biol. Phys. **56**(1):136-144, 2003.

2. The ARTSCAN Protocol. Onkologiskt centrum, Norrlands Universitetssjukhus, Umeå.

3. Bortfeld T and Schlegel W. *Optimization of Beam Orientations in Radiation Therapy: Some Theoretical Considerations.* Phys. Med. Biol. **38**:291-304, 1993.

4. Bortfeld et al. *http://www.aapm.org/meetings/99AM/pdf/2796-50260.pdf,* 1999.

5. Bortfeld et al. *http://www.isye.gatech.edu/nci-nsf.orart.2002/pdf-files/Bortfeld2.pdf,* 2002.

6. Brahme A, Roos J-E and Lax I. *Solution of an Integral Equation Encountered in Rotation Therapy.* Phys. Med. Biol. **27**(10):1221-1229, 1982.

7. Brahme et al. Accuracy Requirements and Quality Assurance of External Beam Therapy with Photons and Electrons. Acta Oncologica, Supplementum 1, 1988.

8. Brahme A, Nilsson J and Belkic D. *Biologically Optimized Radiation Therapy.* Acta Oncologica **40**(6):725-734, 2001.

9. Byrd R H, Lu P, Nocedal J and Zhu C. *A Limited Memory Algorithm for Bound Constrained Optimization.* SIAM Journal on Scientific Computing **16**:1190-1208, 1995.

10. Bäck A. *Intensity Modulated Radiation Therapy in the Head and Neck Region using Dynamic Multi-Leaf Collimation.* Doctorial Thesis, Department of Radiation Physics Gothenburg University, ISBN 91-628-5628-6, 2003.

11. Chui C-S and Spirou S V. *Inverse Planning Algorithms for External Beam Radiation Therapy.* Medical Dosimetry **26**(2):189-197, 2001.

12. Convery D J and Rosenbloom M E. *The Generation of Intensity-Modulated Fields for Conformal Radiotherapy by Dynamic Collimation.* Phys. Med. Biol. **37**(6):1359-1374, 1992.

13. Dawson L A, Anzai Y, Marsh L, Martel M K, Paulino A, Ship J A and Eisbruch A. *Patterns of Local-Regional Recurrence Following Parotid-Sparing Conformal and Segmental Intensity Modulated Radiotherapy for Head and Neck Cancer.* Int. J. Radiation Oncology Biol. Phys. **46**(5):1117-1126, 2000.

14. Deasy J O. *Multiple Local Minima in Radiotherapy Optimization Problems with Dose-Volume Constraints.* Medical Physics **24**(7):1157-1161, 1997.

15. Eisbruch A, Ten Haken R K, Kim H M, Marsh L H and Ship J A. *Dose, Volume, and Function Relationships in Parotid Salivary Glands Following Conformal and Intensity Modulated Irradiation of Head and Neck Cancer.* Int. J. Radiation Oncology Biol. Phys. **45**(3):577-587, 1999.

16. Eisbruch A, Kim H M, Terrell J E, Marsh L H, Dawson L A and Ship J A. *Xerostomia and its Predictors Following Parotid-Sparing Irradiation of Head-and-Neck Cancer.* Int. J. Radiation Oncology Biol. Phys. **50**(3):695-704, 2001.

17. Galvin J M, Chen X-G and Smith R M. *Combining Multileaf Fields to Modulate Fluence Distributions.* Int. J. Radiation Oncology Biol. Phys. **27**:697-705, 1993.

18. Hansen O, Overgaard J, Sand Hansen H, Overgaard M, Hoyer M, Jorgensen K E, Bastholt L and Berthelsen A. *Importance of Overall Treatment Time for the Outcome of Radiotherapy of Advanced Head and Neck Carcinoma: Dependency on Tumour Differentiation.* Radiotherapy and Oncology **43**:47-51, 1997.

19. Horiot J-C, Bontemps P, van den Bogaert W, Le Fur R, van den Weijngaert D, Bolla M, Bernier J, Lusinchi A, Stuschke M, Lopez-Torrecilla J, Begg A C, Pierart M and Collette L. *Accelerated Fractionation (AF) Compared to Conventional Fractionation (CF) Improves Loco-Regional Control in the Radiotherapy of Advanced Head and Neck Cancers: Result of the EORTC 22851 Randomized Trial.* Radiotherapy and Oncology **44**:111-121, 1997.

20. International Commission on Radiation Units and Measurements (ICRU). *Prescribing, Recording, and Reporting Photon Beam Therapy.* ICRU Report 50. Bethesda MD, USA, 1993.

21. International Commission on Radiation Units and Measurements (ICRU). *Prescribing, Recording, and Reporting Photon Beam Therapy (Supplement to ICRU Report 50).* ICRU Report 62. Bethesda MD, USA, 1999.

22. Källman P, Ågren A and Brahme A. *Tumour and Normal Tissue Responses to Fractionated non-Uniform Dose Delivery.* Int. J. Radiation Biology **62**(2):249-262, 1992.

23. La, Sonny. *Dosimetric Verification of Intensity Modulated Radiotherapy Treatment Plans with Radiographic Film.* Master of Science Thesis, Department of Medical Radiation Physics, The Jubileum Institute, Lund University, 2004.

24. MDS Nordion. *DC Algorithms, OTP 1.2.* Document ID: OP-012-MCU-GB_DC-ALGv1.doc.

25. Manning M A, Wu Q, Cardinale R M, Mohan R, Lauve A D, Kavanagh B D, Morris M M and Schmidt-Ullrich R K. *The Effect of Setup Uncertainty on Normal Tissue Sparing with IMRT for Head-and-Neck Cancer.* Int. J. Radiation Oncology Biol. Phys. **55**(5):1400-1409, 2001.

26. Mijnheer B J, Battermann J J and Wambersie A. *What Degree of Accuracy is Required and can be Achieved in Photon and Neutron Therapy.* Radiotherapy and Oncology **8**:237-252, 1987.

27. Mohan R, Wu Q, Manning M and Schmidt-Ullrich R. *Radiobiological Considerations in the Design of Fractionation Strategies for Intensity-Modulated Radiation Therapy of Head and Neck Cancers.* Int. J. Radiation Oncology Biol. Phys. **46**(3):619-630, 2000.

28. Mu X, Löfroth P-O, Karlsson M and Zackrisson B. *The Effect of Fraction Time in Intensity Modulated Radiotherapy: Theoretical and Experimental Evaluation of an Optimization Problem.* Radiotherapy and Oncology **68**:181-187, 2003.

29. Oelfke U and Bortfeld T. *Inverse Planning for Photon and Proton Beams.* Medical Dosimetry **26**(2):113-124, 2001.

30. Samuelsson A and Johansson K-A. *Intensity Modulated Radiotherapy Treatment Planning for Dynamic MLC Delivery: Influence of Different Parameters on Dose Distributions.* Radiotherapy and Oncology **66**(1):19-28, 2003a.

31. Samuelsson A, Mercke C and Johansson K-A. *Systematic Set-up Errors for IMRT in the Head and Neck Region: Effect on Dose Distribution.* Radiotherapy and Oncology **66**(3):303-311, 2003b.

32. SBU-rapport nr 129/2. *Strålbehandling vid cancer*. Statens beredning för utvärdering av medicinsk metodik (The Swedish Council on Technology Assessment in Health Care), ISBN: 91-87890-33-X, 1996.

33. SBU-rapport nr 162/1. *Strålbehandling vid cancer*. Statens beredning för medicinsk utvärdering (The Swedish Council on Technology Assessment in Health Care), ISBN: 91-87890-82-8, 2003.

34. Saw C B, Siochi R A C, Ayyangar K M, Zhen W, Enke C A. *Leaf Sequencing Techniques for MLC-based IMRT.* Medical Dosimetry **26**(2):199-204, 2001.

35. Smith S, and Lasdon L. *Solving Large Sparse Nonlinear Programs Using GRG*. ORSA Journal on Computing **4**(1), 1992.

36. Stein J, Mohan R, Wang X-H, Bortfeld T, Wu Q, Preiser K, Ling C C and Schlegel W. *Number and Orientations of Beams in Intensity Modulated Radiation Treatments.* Medical Physics **24**(2):149-160, 1997.

37. Söderström S and Brahme A. *Which is the Most Suitable Number of Photon Beam Portals in Coplanar Radiation Therapy?* Int. J. Radiation Oncology Biol. Phys. **33**(1):151-159, 1995.

38. Söderström S, Eklöf A and Brahme A. *Aspects on the Optimal Photon Beam Energy for Radiation Therapy.* Acta Oncologica **38**(2):179-187, 1999.

39. Wang J Z, Li X A, D'Souza W D and Stewart R D. *Impact of Prolonged Fraction Delivery Times on Tumour Control: A Note for Intensity-Modulated Radiation Therapy (IMRT).* Int. J. Radiation Oncology Biol. Phys. **57**(2):543-552, 2003.

40. Webb S. *Optimisation of Conformal Radiotherapy Dose Distributions by Simulated Annealing.* Phys. Med. Biol. **34**(10):1349-1370, 1989.

41. Wu Q, Manning M, Schmidt-Ullrich R and Mohan R. *The Potential for Sparing of Parotids and Escalation of Biologically Effective Dose with Intensity Modulated Radiation Treatments of Head and Neck Cancers: A Treatment Design Study.* Int. J. Radiation Oncology Biol. Phys. **46**(1):195-205, 2000.

42. Wu Q and Mohan R. *Multiple Local Minima in IMRT Optimization Based on Dose-Volume Criteria.* Medical Physics **29**(7):1514-1527, 2002.